

# Renal Biology Driven Macro- and Microscale Design Strategies for Creating an Artificial Proximal Tubule Using Fiber-Based Technologies

IJsbrand M. Vermue,<sup>■</sup> Runa Begum,<sup>■</sup> Miguel Castilho, Maarten B. Rookmaaker, Rosalinde Masereeuw, Carlijn V. C. Bouten, Marianne C. Verhaar, and Caroline Cheng\*

Cite This: *ACS Biomater. Sci. Eng.* 2021, 7, 4679–4693

Read Online

ACCESS |

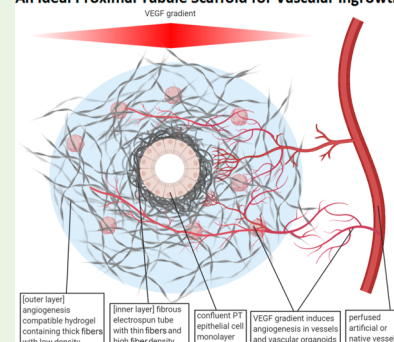
Metrics & More

Article Recommendations

**ABSTRACT:** Chronic kidney disease affects one in six people worldwide. Due to the scarcity of donor kidneys and the complications associated with hemodialysis (HD), a cell-based bioartificial kidney (BAK) device is desired. One of the shortcomings of HD is the lack of active transport of solutes that would normally be performed by membrane transporters in kidney epithelial cells. Specifically, proximal tubule (PT) epithelial cells play a major role in the active transport of metabolic waste products. Therefore, a BAK containing an artificial PT to actively transport solutes between the blood and the filtrate could provide major therapeutic advances. Creating such an artificial PT requires a biocompatible tubular structure which supports the adhesion and function of PT-specific epithelial cells. Ideally, this scaffold should structurally replicate the natural PT basement membrane which consists mainly of collagen fibers. Fiber-based technologies such as electrospinning are therefore especially promising for PT scaffold manufacturing. This review discusses the use of electrospinning technologies to generate an artificial PT scaffold for *ex vivo/in vivo* cellularization. We offer a comparison of currently available electrospinning technologies and outline the desired scaffold properties required to serve as a PT scaffold. Discussed also are the potential technologies that may converge in the future, enabling the effective and biomimetic incorporation of synthetic PTs in to BAK devices and beyond.

**KEYWORDS:** proximal tubule, scaffolds, electrospinning, artificial kidney, basement membrane

An Ideal Proximal Tubule Scaffold for Vascular Ingrowth



## 1. INTRODUCTION

Kidney function can be summarized as the homeostatic regulation of the water volume and solute content in the blood. This is achieved through three processes (filtration, secretion, and reabsorption) all of which are executed in the nephrons (Figure 1a).<sup>1</sup> Solute exchange between the blood and the filtrate consists of passive and active transport. The latter is executed by membrane transporters of epithelial cells located in the tubules of the nephron (Figure 1b). In the case of end stage renal disease (ESRD), these processes are disrupted and unable to maintain homeostatic solute levels and fluid volume, resulting in major health complications. Recent technological advancements have the potential to reintegrate renal tubular functions to ESRD patients without using a donor kidneys.

Just in 2016 alone, over half a million Europeans received renal replacement therapy due to end stage kidney disease (ESKD). While kidney transplantation is the preferred treatment, the majority of ESKD patients receive hemodialysis (HD) or peritoneal dialysis due to a scarcity of donor kidney grafts.<sup>2</sup> Patients who receive HD have a 5 year survival probability below 50%, which is significantly less than patients

who received a kidney transplant (>90%).<sup>2</sup> An important factor responsible for this high mortality is that HD does not include excretion of large lipophilic and protein bound solutes,<sup>3–8</sup> leading to the accumulation of large protein-bound uremic toxins (Figure 1b), which are associated with an increased risk of cardiovascular disease.<sup>9–12</sup>

A bioartificial kidney (BAK) device could offer a promising solution to the complications seen in current dialysis methods.<sup>3–5,13</sup> Essentially, the BAK could further expand on the existing dialysis techniques by incorporating kidney tubule epithelial cells that would also enable the active transport of solutes, including some of the human serum albumin-bound uremic toxins such as indoxyl sulfate and kynurenic acid, between the blood and the dialysate, thereby facilitating their removal.<sup>14</sup> Although the ideal solution would be to grow

Received: March 25, 2021

Accepted: August 24, 2021

Published: September 7, 2021



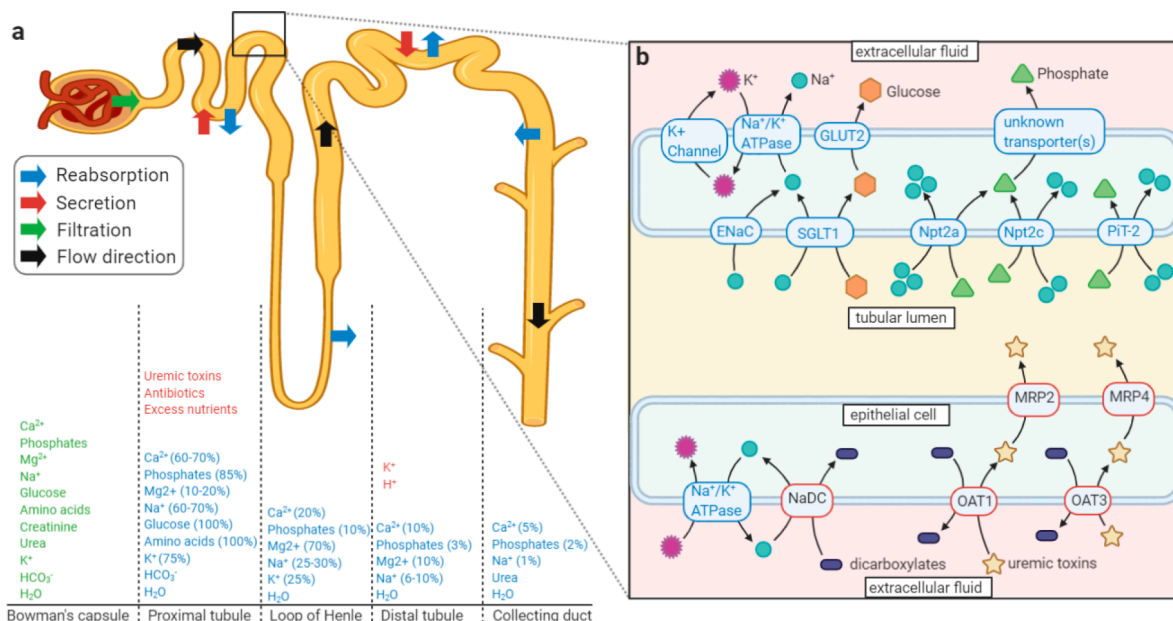


**Figure 1.** Schematic representation of the nephron and active transport mechanisms in the proximal tubule. (a) A schematic figure showing all segments of the nephron: Bowman's capsule, proximal tubule, loop of Henle, distal tubule, and collecting duct. The three kidney processes are color coded: filtration (green), secretion (red), and reabsorption (blue). For each process, examples of solutes are given in the corresponding color. Reabsorbed solutes show a percentage that represents how much of the total reabsorption is performed by that nephron segment. (b) Apical and basolateral membrane transporters in the proximal tubule involved in reabsorption and secretion of solutes. The transport of phosphate and uremic toxins is highlighted to indicate that they are not sufficiently removed by HD. The concentration gradients that result from this active transport give rise to passive transport of fluid and ions through osmosis and diffusion: epithelial Na<sup>+</sup> channel (ENaC), Na<sup>+</sup>-glucose cotransporter (SGLT1), facilitated glucose diffusion transporter (GLUT2), sodium-dependent phosphate transport protein (Npt2a, Npt2c, PiT-2), divalent anion-sodium symporter (NaDC), organic anion transporter (OAT1, OAT3), multidrug resistance-associated protein 2 (MRP2, MRP4).

transplantable kidney tissue in the laboratory,<sup>15</sup> the bioartificial approach seems a more readily achievable solution and has already been studied in clinical trials.<sup>16</sup> Given the complexity of the kidney and its many functional roles, it is likely that a BAK device would incorporate multiple synthetic functional units in order to address the current shortcomings in treatment options.<sup>16,17</sup> Each functional unit may be derived from different fabrication methods in order to cater to specific cellular and/or metabolic needs.

Over a decade ago Humes et al. showed the beneficial effects of using renal tubular cells on polymeric scaffolds in combination with dialysis in patients with acute kidney injury.<sup>18,19</sup> More recent iterations of this approach have successfully incorporated a bioartificial renal epithelial cell system (BRECS) in a continuous flow peritoneal dialysis circuit.<sup>20</sup> The BRECS consists of a bioreactor that houses porous, niobium-coated carbon disks on which adult human renal epithelial cells are grown *in vitro*. Once the optimal cell density is reached, the disks can be clinically perfused either with ultrafiltered blood or peritoneal fluid from extracorporeal HD or peritoneal dialysis circuits. In combination with the latter, this strategy could be further developed into a portable BAK system that greatly improves the quality of life for the patient. A 65 kDa molecular weight cutoff in pre- and postcell filters achieves immune-isolation and protection of the BRECS epithelial cells while also permitting the secretion of small proteins and hormones to the patient's blood circulation. Another BAK approach for restoring renal tubular function to the patient is the implantation of artificial renal tubules.<sup>21</sup> Although at an early stage, proof of concept studies have already been performed and show proximal tubule epithelial cells (PTEC) can remain functional for at least 3 weeks *in*

*vitro*.<sup>22</sup> PTECs are especially interesting for these studies because the proximal tubule (PT) naturally contributes to the secretion of the large protein bound uremic toxins that are insufficiently removed by HD (Figure 1). Finding the optimal scaffold parameters for creating a functional artificial PT has been the focus of various studies.<sup>14,22–27</sup>

Incorporating PTECs in a BAK requires a supporting structure that enables cells' natural function. In the native kidney, PTEC are attached to the basement membrane (BM). The PTEC form a confluent monolayer, essential for achieving solute concentration differences between the filtrate and the blood. The BM consists mostly of nanosized fibers composed of natural polymers like collagen. These fibers are organized in a fibrous network that is permeable to the solutes that are transported by the PTECs. Although it is possible to extract the BM from human kidneys, this would again face the issue of limited availability.<sup>28</sup> In an alternative route, the therapeutic potential of decellularized kidneys sourced from animals has also been investigated. *In vitro* studies show decellularized extra-cellular matrix has the potential to support cells and direct cell fate, but *in vivo* tests have thus far had limited success due to immune reactivity and thrombosis.<sup>29,30</sup> Artificially produced fiber-based scaffolds offer off-the-shelf availability and clinical grade biodegradable materials and can be tuned to specific nano- and macroscale properties, such as fiber diameter, porosity, and scaffold thickness.<sup>31–33</sup> Artificial scaffolds have already been investigated for their ability to support a functional confluent PTEC monolayer. Among the methods to generate fiber scaffolds, electrospinning is a versatile and low cost technology that can be employed to generate fiber-based structures using a variety of natural and synthetic biodegradable materials at both nano- and micro-

Table 1. Summary of Electrospinning Types

electrospinning type	advantages	disadvantages
solution electrospinning	<ul style="list-style-type: none"> <li>- simple setup</li> <li>- low solution viscosity allows for thin dispensing nozzels to be used, enabling nanofiber fabrication</li> <li>- low distance/voltage setups are capable of electrospinning live cells</li> </ul>	<ul style="list-style-type: none"> <li>- involves (toxic) solvents</li> <li>- high voltage limits use of live cells</li> </ul>
melt electrospinning	<ul style="list-style-type: none"> <li>- no (toxic) solvents required</li> <li>- random (MES) or controlled (MEW) fiber deposition possible</li> </ul>	<ul style="list-style-type: none"> <li>- high solution viscosity requires wide dispensing nozzle, limiting nanofiber production</li> <li>- fabrication process relatively complex due to heating elements</li> <li>- heat requirement limits material compatibility</li> <li>- limited commercial availability</li> <li>- high voltage limits use of live cells</li> </ul>
near-field electrospinning	<ul style="list-style-type: none"> <li>- material compatibility</li> <li>- controlled fiber deposition</li> <li>- low voltage</li> <li>- supports electrospinning of live cells/bacteria, maintaining viability</li> </ul>	<ul style="list-style-type: none"> <li>- nanofiber fabrication is relatively difficult</li> <li>- limited scaffold thickness</li> </ul>

scale. Relative to other fiber fabrication methods, such as phase separation or self-assembly, electrospinning methods, specifically melt- and near-field electrospinning, afford the user both spatial and temporal control in 3D material design.<sup>34</sup>

The ideal PT scaffold not only supports PTECs on the luminal side but also stimulates close integration of vasculature on the abluminal side. This allows connection to the host's vasculature and opens the technology toward a continuously active intracorporeal BAK. Therefore, a PT scaffold should support and promote both renal membrane and vascular structure formations. Electrospinning has already shown its potential in other fields, such as cardiovascular tissue engineering.<sup>33,35,36</sup> In theory, this technique can be used to fabricate customized fiber-based renal tubular scaffolds, using a variety of materials. However, dedicated studies on electrospinning of renal scaffolds that can support PT cell growth, differentiation, and vascular structure formation are scarce. Additionally, only a handful of studies focused on reabsorptive/secretory function or clinical implementation (Table 1). In contrast the most advanced electrospun vascular scaffolds in the cardiovascular field already offer combinations of fiber networks with bioactive materials that can support multiple vascular cell types.<sup>33,37</sup> For example, the vascular scaffold produced by Han et al.<sup>33</sup> contained separate layers and growth factors to optimally support EC growth on the luminal side and vSMC growth on the outside of the construct. In a similar fashion the ideal PT scaffold would give optimal support for PTECs on the luminal side of the scaffold while supporting vascular integration in a second layer on the abluminal side. In addition to supporting both renal and vascular structures, the construct should minimize the distance between the two in order to optimize solute exchange. For reference, the distance between the PT and capillaries in native renal tissue is roughly 5  $\mu\text{m}$  *in vivo*. In addition, the successful implementation of fiber scaffolds into the renal regenerative field requires an understanding of the biological response to the native BM. By taking aspects of the natural renal BM into consideration, optimal biological viability and function may be achieved and greatly advance the next generation of artificial kidney tubules. This review will discuss the properties of the BM and the application of electrospinning in artificial PTs and propose a possible strategy for optimizing vascular integration and BM mimicry.

## 2. NATURAL PROXIMAL TUBULE BASEMENT MEMBRANE AND ARTIFICIAL BIOMIMICRY

One of the hurdles to designing an artificial PT is creating a replacement for the BM on which the PTECs are anchored. The PT BM, part of the extracellular matrix (ECM), is a fiber-based sheetlike network that offers structural support to the adhering cells and plays an integral role in cell signaling and cell fate, while allowing solute and water exchange with the surrounding tissue. The epithelial cells deposit BM components while also releasing factors that degrade these components, resulting in constant BM remodeling. Although information on the turnover rate of the tubular BM is limited, it has been suggested to be in the range of multiple weeks.<sup>38</sup> In theory, the artificial scaffold for replacement of the BM should ideally be fully degradable, to allow adaptation of BM to changes in *in situ* conditions (such as changes in blood or filtrate flow) after implantation by natural remodeling.

**2.1. Proximal Tubule Basement Membrane.** Many factors like the biological cues provided by BM proteins and mechanical properties should be taken into account for the design of an artificial replacement of the BM. The main components of the BM are collagen IV, laminins, nidogens, and heparan sulfate proteoglycans (HSPGs).<sup>24,39,40</sup> Collagen IV has a triple helical structure that forms a cross-linked fiber-based network, which contributes significantly to the renal tubular BM stiffness.<sup>40</sup> Collagen microfibrils can wrap around each other to form collagen fibers, which vary in diameter ranging from 10 to 300 nm.<sup>41</sup> Considering the low mechanical stress in the kidney tubules, the collagen fibers in the PT BM are most likely thin. Similar to collagen IV, laminins assemble into a network and contribute to the mechanical integrity of the basement membrane.<sup>42,43</sup> The laminin network plays a role in cell anchoring by binding to plasma membranes such as integrins.<sup>44</sup> Ultrahigh resolution scanning electron microscopy reveals that the tubular BM surface is covered in parallel cristae with "hills" of approximately 50 nm wide which consists of a meshwork of fibers that are 7 nm wide and up to 100 nm long.<sup>45</sup> The collagen and laminin networks are connected through nidogens and HSPGs, the latter of which also serve as reservoirs for growth factors,<sup>46</sup> are highly hydrated, and contribute to a negatively charged barrier within the BM.<sup>45,47,48</sup> A negative surface potential is crucial, as it strengthens the adhesion capabilities of human embryonic kidney cells.<sup>49</sup> The renal tubular BM thickness has been estimated to be 360–558 nm.<sup>50–52</sup> Although no data is



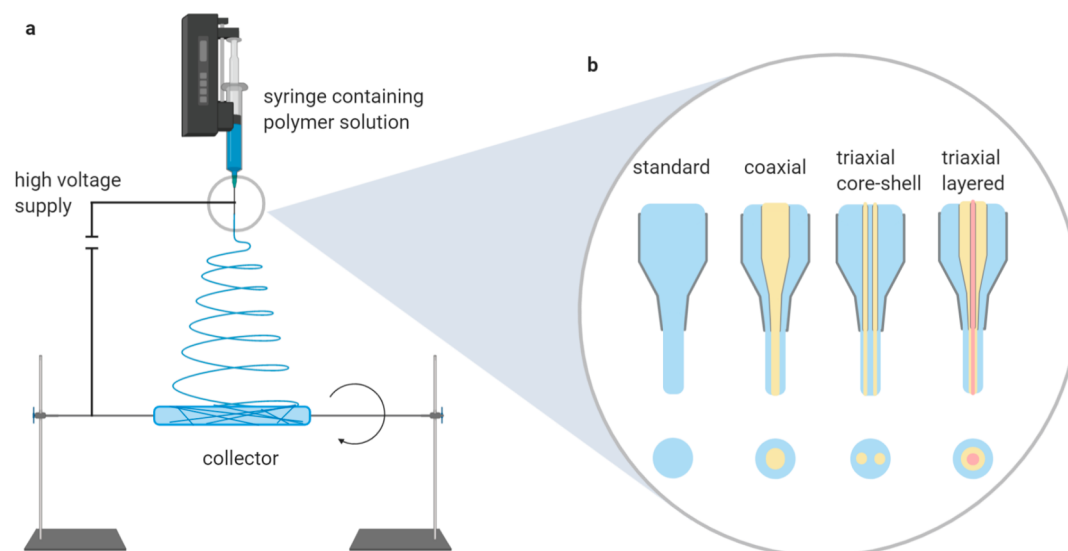


**Figure 2.** Schematic representation of an electrospinning device for tubular construct fabrication. (a) Schematic summary of the electrospinning process. A rotating rod is used as a collector to create tubular scaffolds. (b) Possible spinneret modifications for the production of fibers containing multiple materials. Coaxial/triaxial electrospinning can be used to produce fibers with different material layers.

available concerning the mechanical properties of these structures, measurements of BM derived from chicken retina with a similar thickness have reported a Young's modulus of 3.34–3.57 MPa.<sup>53</sup> It should be noted that the composition and properties of the BM may vary between different tissues and species<sup>42</sup> and that under physiological conditions the BM is supported by surrounding tissue and fluid pressures that increase its stiffness. Furthermore, the effect of substrate stiffness on the viability of renal proximal tubular epithelial cells has been analyzed in the range of 0.1–20 kPa, which is more in line with the stiffness of the kidney as a whole<sup>54</sup> and showed that the cells performed better when exposed to a higher substrate stiffness.<sup>55</sup> Taking the aforementioned properties of the BM into consideration, certain key criteria should be taken into account when we strive to design the optimal PT scaffold. First, scaffolds designed to mimic the PT BM should optimally support PT epithelial cells in their transport function. The scaffold should enable the PT cells to adhere to the scaffold and stimulate cell-junction formation with each other, thus generating a confluent monolayer. Investigating which type of integrin subunits are highly expressed and which integrin forms are more active on PT epithelial cells as well as assessing their integrin response to macro and nanoscale variables of an artificial scaffold would greatly aid in optimizing scaffold design for cell adhesion.<sup>56</sup> Second, the scaffold should also be permeable to solutes involved in the secretion and reabsorption mechanisms performed by the PT. For this, the creation of the confluent PT epithelial layer is critical to establish a selectively permeable border and similarly relies on optimizing the interaction between scaffold fiber and integrin-mediated cell adhesion. Finally, as discussed above, scaffold thickness should be minimal in order to maximize the efficiency of solute exchange between the artificial PT and surrounding vasculature.

**2.2. Fabricating an Artificial Proximal Tubule Basement Membrane.** Fiber-based technologies are highly suitable to generate an artificial PT BM scaffold that can replicate native BM function. This class of manufacturing technologies includes a range of solvent and thermal-based electrodriven fiber formation methods capable of creating

ECM-mimicking fibrous scaffolds. Electrospinning enables the processing of a wide range of polymeric materials, and the encapsulation of growth factors or bioactive molecules in order to optimize cell performance. Polymers suitable for electrospinning and currently used in various (pre)clinical applications can be divided into natural polymers such as fibroin (silk), collagen (gelatin), chitosan (CS), hyaluronic acid (HA), and elastin and synthetic polymers such as poly( $\epsilon$ -caprolactone) (PCL), poly(L-lactide-co- $\epsilon$ -caprolactone) (PLCL), poly lactic acid (PLA), poly(3-hydroxybutyrate) (PHB), and polyurethane (PU).<sup>31,35,57,58</sup> Furthermore, electrospun structures may be coated or encapsulate growth factors or bioactive molecules in order to optimize cell performance.<sup>33</sup>

Fiber-based technologies include several manufacturing processes from which the most investigated are solution electrospinning (SES), melt electrospinning (MES), melt electrowriting (MEW), and near-field spinning (NFES), each of which has their pros and cons in terms of setup complexity, deposition accuracy, material compatibility, and fiber diameter (Table 1). These fiber-based technologies all allow for the development of fiber-based scaffolds with a wide variety of design parameters.<sup>59</sup> Altering certain parameters during production or postprocessing allows for precise control over the mechanical properties,<sup>35</sup> scaffold thickness,<sup>58</sup> degradation speed,<sup>60</sup> fiber size,<sup>31</sup> fiber orientation,<sup>61</sup> material composition,<sup>22,33</sup> pore size,<sup>62,63</sup> biological cues,<sup>22,33,64</sup> and growth factor gradients.<sup>35,58</sup> Although electrospun scaffolds are relatively new for the field of kidney tissue engineering,<sup>22</sup> they have been widely investigated for skin, muscle, cartilage, bone, nerve, and blood vessel applications.<sup>31,35,65</sup>

**2.2.1. Customizable Fiber-Based Scaffolds.** An electrospinning device consists of a syringe containing a polymer solution, a high voltage supply and an electrically conductive collector (Figure 2a). The voltage supply is used to create an electric potential between the dispensing nozzle and the collector. When the electrical field overrules the surface tension of the charged solution at the tip of the spinneret, the solution forms a jet that is pulled toward the oppositely charged collector. The charged jet accelerates by and in the direction of the electric field with a whipping motion.<sup>66</sup> While traveling

Table 2. Summary of Studies Using Kidney Epithelial Cells on Electrospun Scaffolds<sup>a</sup>

material(s)	fiber diameter ( $\mu\text{m}$ )	coating/alignment	cell type	mechanical properties	evaluated parameters	results	ref
PCL	0.53–1.06	L-DOPA and collagen	iREC, ciPTEC	TM: 16.5–67.7 MPa SaB: 20–80%	secretion capability and monolayer formation, ZO1 expression	both mechanisms were present, except when seeding iREC on large pore size scaffolds	21
Ury-PCL and Ury-urea-PCL	0.34–0.44	n.a.	HK-2	n.a.	transporter expression, flow exposure, ZO1 expression and monolayer formation	flow stimulates epithelial phenotype and protein content, monolayer present	70
PLA	0.88–3.71	n.a.	PRK	YM: 0.57–8.69 MPa UTS: 0.87–4.25 MPa	cell viability, cell phenotype, fiber diameter effect	viable multicell population, fiber diameter does not impact viability	71
polyamide	0.18	n.a.	NRK	n.a.	actin and integrin expression, proliferation	compared to the glass control actin expression and proliferation increased 50%, integrin localization changed	72
CS, collagen, and PCL	0.2–0.55	aligned/random	MDBK	n.a.	actin synthesis, cell morphology	cells align with the fiber direction and actin synthesis is increased in the presence of collagen	59
PHB	0.993	n.a.	Vero	YM: 4.7 MPa SaB: 12%	cell attachment, cell proliferation	increased proliferation on SES scaffold compared to salt-leached scaffold	73
CS, PCL, and HA	0.362	n.a.	Vero	YM: 16–26 MPa SaB: 35–115%	actin expression, cell viability	incorporating HA on a CS-PCL scaffold increases Vero viability and actin expression	65
PCL and dKECM	0.383–0.4	n.a.	HK-2	YM: 6.7–25.42 MPa	ZO1 expression, metabolic activity, cell proliferation, monolayer formation	cell performance increased with dKECM content, ZO1 not expressed in absence of dKECM	74
fibroin	n.a.	aligned	CKT	n.a.	adhesion, cell growth	increased adhesion and decreased cell growth when compared to thermanox control	75
PHMB loaded PLA	0.565–1.565	n.a.	MDCK	n.a.	antibacterial properties, biocompatibility	cells remained viable with a PHMB content below 1.5 wt %	76
PCL	3.68	n.a.	MDCK	n.a.	monolayer formation	monolayer not formed	66
PCL	0.418	protein adsorption	Vero	n.a.	cell viability	cell viability is higher on a 0.6 mm thick scaffold than a 0.1 mm thick scaffold	67
PCL	0.95–5.35	aligned/random	RC-124	YM: 0.17–36 MPa SaB: 0.81–9.36%	cell viability, gene expression	cell viability not impacted by fiber diameter, PT associated gene upregulated compared to TCPS	68
PHB	2.4–5.9	n.a.	HEK 293	n.a.	cytotoxicity	PHB is not cytotoxic	69

<sup>a</sup>All experiments were performed *in vitro* and all scaffolds were made using SES. Fiber diameters and mechanical properties are averages; a range is given when multiple scaffolds are used. PCL poly( $\epsilon$ -caprolactone), iREC induced renal tubular epithelial cells (murine), ciPTEC urine-derived proximal tubule epithelial cells (human), TM tangent modulus, SaB strain at break, Ury ureidopyrimidinone, HK-2 human kidney 2 epithelial cells, n.a. not available, because it is not measured or not used, PLA poly(lactic acid), PRK primary rat kidney cells, YM Young's modulus, UTS ultimate tensile strength, NRK normal rat kidney cells, CS chitosan, MDBK madine darby bovine kidney cells, PHB poly(3-hydroxybutyrate), Vero monkey epithelial kidney cells, HA hyaluronic acid, dKECM decellularized kidney extracellular matrix, CKT chicken kidney tissue, PHMB polyhexamethylenebiguanide hydrochloride, MDCK madin darby canine kidney cells, RC-124 human kidney primary epithelial cell line, TCPS± tissue culture polystyrene, HEK 293 human embryonic kidney 293 cells.

toward the collector, the volatile solvent evaporates, resulting in the deposition of a continuous polymer fiber.<sup>35</sup> A wide range of accessories, consisting mostly of spinnerets and collectors, have been investigated to suit application needs and rotating mandrels have been utilized as collectors to form tubular scaffolds, as illustrated in Figure 2a. In addition to this, there are different parameters available to tune the properties of the scaffold to suit its purpose: spinneret to collector distance, applied voltage, polymer concentration, polymer molecular weight, solvent choice, and more. These parameters and their influence on the product traits are aptly described in different reviews.<sup>31,35</sup> Production of thinner fibers may be achieved by decreasing polymer concentration, flow rate, and or by increasing the voltage and solution conductivity. Furthermore, hollow fiber structures or multilayered fibers consisting of multiple materials can be produced by using multiaxial core-shell spinneret designs (Figure 2b). Using multilayered, multimaterial fibers can be an effective way to drastically alter the mechanical properties, cell-surface interactions, growth factor release, or degradation speed of the scaffold.<sup>33,35,67</sup> Although this does often lower the efficiency of nanofiber generation, it can enable the fabrication of multilayered materials with distinct architectures per layer.

**2.2.2. Electrospinning Artificial Proximal Tubules.** Although research concerning electrospinning for the generation of a PT scaffold is relatively scarce and thus far has only reported the use of SES, the advances made toward application are significant. Solution electrospinning has been implemented in PT cell culture using various materials, fiber diameters, and cell sources (Table 2). Different materials including PCL, CS, fibroin, PLA, and PHB have been used, with fiber diameters ranging from 0.18 to 5.9  $\mu\text{m}$ .<sup>22,61,75-78,67-74</sup> In terms of fiber architectures, most studies reported on random fiber deposition instead of aligned fibers. The resulting scaffolds present a Young modulus ranging from 0.17 to 36 MPa.

PCL is one of the most widely studied electrospun materials for use as a PT scaffold. The versatility of this synthetic polymer is owed to, among others, its biocompatible, biodegradable, and elastic properties.<sup>79,80</sup> However, its hydrophobic nature requires the use of a biological coating to support cell adhesion and proliferation. L-DOPA and collagen coated PCL has shown its potential in a proof of concept study performed by Jansen et al.,<sup>22</sup> where 12, 16, and 20% PCL solutions were used to create the fiber-based scaffolds resulting in a fiber diameter of  $0.53 \pm 0.30$ ,  $0.88 \pm 0.44$ , and  $1.06 \pm 0.66$   $\mu\text{m}$ , respectively. These scaffolds had an inner diameter of 700  $\mu\text{m}$  and were seeded with either murine induced renal tubular epithelial cells (iREC) or human conditionally immortalized proximal tubule cells (ciPTEC), which had a cell size of  $13.7 \pm 1.3$  and  $29.7 \pm 5.5$   $\mu\text{m}$ , respectively. Even though the 12% solution scaffold showed beading artifacts, this scaffold allowed iREC cells to develop a monolayer with increased expression of Zona Occludens 1 (ZO1), a tight junction marker, due to its smaller fiber size. ciPTECs were larger in size and therefore able to form a monolayer on scaffolds obtained from the three polymer concentrations. The epithelial monolayers in the scaffolds showed active transport through OAT1 and OAT2 transporters indicating the potential of coated PCL scaffolds for the development of functional PT grafts. Other studies have shown PCL fibers can also be deposited in an aligned form instead of random, causing the kidney cells to stretch out in the direction of the fibers and increase their F-actin synthesis.<sup>61</sup> In addition to a collagen coating, SES of a HA

layer on top of a CS/PCL hybrid also appears to increase cell viability and actin filament production in monkey kidney epithelial cells *in vitro*.<sup>67</sup> Instead of coating the PCL using natural polymers, Sobreiro-Almeida et al.<sup>72</sup> have shown that PCL can be mixed with porcine decellularized kidney ECM and subsequently electrospun into a fiber-based scaffold with a fiber diameter of roughly 400 nm. A human proximal tubule epithelial cell line (HK2) seeded on the PCL/ECM structure showed increased metabolic activity, cell proliferation, and protein content when compared to a pure PCL structure. Furthermore, the HK2 cells would only express ZO1 on the PCL/ECM hybrid and showed a significantly higher epithelial barrier function by measuring trans-epithelial electrical resistance.<sup>72</sup> The susceptibility of PCL to enzymatic and oxidative degradation can be altered by incorporating units such as 2-ureido-[1H]-pyrimidin-4-one (UPy) or bis-urea (BU) into the polymer. The resilience gained or lost by incorporating UPy or BU when exposed to various degradation mechanisms was quantified by Brugmans et al.<sup>81</sup> In contrast to conventional PCL scaffolds, the PCL-UPy or PCL-BU scaffolds would actually become stiffer during the degradation process.<sup>60,81</sup> Mollet et al.<sup>68</sup> have used PCL-UPy to create a membrane capable of supporting a confluent layer of ZO1 expressing human kidney 2 epithelial cells (HK-2). The bioreactor used in this study allowed for the separate admission of medium on the apical and basal side of the HK-2/PCL-UPy membrane. Compared to a PCL-UPy scaffold without cells, the HK-2/PCL-UPy construct showed a significant decrease in inulin permeability. Since inulin is neither secreted nor reabsorbed by renal epithelial cells, this indicates the formation of a near-complete epithelial barrier. Additionally, the expression of specific membrane transporters was evaluated under static and flow conditions, which revealed that flow significantly impacts the expression of PEPT1 and PEPT2 at RNA level, while OAT1, OAT3, SGLT2, and Na<sup>+</sup>/H<sup>+</sup> exchanger were not significantly impacted.<sup>68</sup>

Poly lactic acid (PLA) is another well-known biomaterial widely used for SES. Burton et al.<sup>69</sup> produced PLA scaffolds based on 10, 18, and 22% (w/v) solution, resulting in  $0.88 \pm 0.16$ ,  $2.46 \pm 0.43$ , and  $3.30 \pm 0.17$   $\mu\text{m}$  fiber diameters, respectively. These substrates were able to support primary rat kidney cells expressing ductal (Aquaporin-1, Aquaporin-2) and glomerular (von Willebrand factor, Synaptopodin) markers for 7 days. However, they did not witness monolayer organization of the cells within this time frame, which is significant as this, in addition to ZO1 cell junction formation is essential to epithelial barrier function.<sup>82</sup> Llorens et al.<sup>74</sup> have shown that PLA scaffolds can have significantly improved antibacterial properties when including polybiguanide (PHMB) in the polymer solution while maintaining biocompatibility during *in vitro* culture of canine epithelial kidney cells.

### 3. ELECTROSPINNING STRATEGIES FOR VASCULAR GRAFTS TO ADVANCE RENAL SCAFFOLD DESIGN

We have discussed the current uses of electrospinning methods in PT scaffold fabrication, (to date using only solution electrospinning) and highlighted the promising results. However, other research fields that use electrospun scaffolds for (pre)clinical applications, in particular the cardiovascular field, may provide new concepts and solutions to further innovate PT scaffold design. Indeed, the promising results of various advanced electrospun designs are supported by data in which electrospun scaffolds were proven to produce viable and



functional tissue engineered vascular structures *in vitro* and *in vivo*.<sup>33,83</sup> For example Han et al.<sup>33</sup> used a multilayered scaffold which combined four materials and two growth factors to mimic and promote native vessel anatomy. The construct consisted of three layers, an inner layer of poly(ethylene glycol)-*b*-poly(*L*-lactide-*co*- $\epsilon$ -caprolactone) (PELCL) containing vascular endothelial growth factor (VEGF), a middle layer of poly(*L*-lactide-*co*-glycolide) (PLGA) containing platelet-derived growth factor-bb (PDGF), and an outer layer of PCL. A secondary needle was used to spin gelatin fibers throughout each layer, adding to the adhesion properties and enabling cell ingrowth after a short degradation period. PELCL was chosen as the inner layer and carrier of VEGF, because it enables a relatively fast growth factor release when compared to the release of PDGF from the PLGA layer. This promotes rapid endothelialization by initial VEGF release, followed by PDGF induced recruitment of vascular smooth muscle cells for stabilization of the newly formed confluent endothelium. The outer layer of PCL improved the mechanical properties of the construct. In the *in vivo* testing phase scaffolds containing either zero, one or both growth factors were analyzed 4 and 8 weeks after implantation in a rabbit carotid artery. The construct containing both growth factors gave the best results and was not obstructed after 8 weeks *in vivo*, indicating how advanced tuning of scaffold properties can greatly enhance controlled cellularization.<sup>33</sup> In addition to this multilayered approach, many PCL scaffold modifications have been analyzed in order to optimize its biomimetic properties. This includes a vascular graft model containing a luminal layer of electrospun collagen I fibers for increased biocompatibility *in vitro*, but at the cost of mechanical properties,<sup>84</sup> a similarly designed layered scaffold using silk fibroin as luminal material,<sup>85</sup> a PCL/PLGA hybrid resulting in accelerated degradation *in vivo*,<sup>86</sup> a fibronectin coated PCL/PLA and PCL/PLA/PEG hybrid with a significantly improved endothelial adhesion and viability *in vitro* when compared to a gelatin or blood coating,<sup>64</sup> and a coaxially spun fiber with a heparin core and a collagen/chitosan/PLCL shell which was able to release heparin for more than 45 days.<sup>87</sup> Given the effectiveness of layered electrospun scaffolds containing growth factors in vascular tissue engineering, translating these strategies to kidney engineering should be considered. In particular, layered compartmentation of scaffold regions each with either PT epithelium and/or microvasculature promoting abilities, may be the most viable solution when we aim for a design to connect PT tubules with a microvascular bed.

**3.1. Melt Electrospinning/Writing for Proximal Tubule Fabrication.** Different types of electrospinning used in other fields should also be considered for PT scaffolds. In contrast to SES, there is no evaporation of solvent in melt electrospinning (MES) and melt electrowriting (MEW) systems because these use heated spinnerets to electrospin undissolved polymers in their liquid phase. Thus, MES and MEW do not have an evaporation step before deposition on the collector resulting in a generally larger fiber diameter when compared to SES.<sup>58</sup>

MES has not yet been applied to kidney tissue engineering at the time of writing. Various aspects of MES may contribute to this. First, fiber diameters are relatively large when compared to SES and may require more complex setups (such as modified spinnerets<sup>88</sup>) to create fibers in the nanometer range. This is further complicated by the limited number of commercially available MES devices.<sup>58</sup> Second, the heating

required to reduce fiber diameter limits the use of natural polymers which are thermosensitive, such as chitosan.<sup>58</sup> Third, the viscosity of the molten polymer used is a full magnitude higher than SES due to the absence of solvent, which poses limitations for the flow rate at the dispensing nozzle and thus fiber diameter size.<sup>89</sup> Finally, difficulties with obtaining a consistent fiber diameter have been reported, especially in the submicrometer range.<sup>58,90</sup>

Melt electrowriting (MEW) is related to MES but has the great advantage that it can precisely deposit fibers, which can have a significant impact on cell responses such as alignment, intercellular mechanical stress distribution and sensing, as well as subsequent transcriptional response.<sup>49,91</sup> Similar to MES, MEW uses polymer melts instead of polymer solutions and small collecting distances to develop well-organized fiber-based scaffolds. By using computer-controlled translation and rotation of the collector, MEW is capable of precisely depositing polymer fibers in organized scaffolds up to 7 mm thick. These qualities make MEW a suitable production method for large macrovessel scaffolds for replacement of, e.g., the large caliber coronary vessels or vascular access graft.<sup>31,59</sup> It has also been suggested as a suitable option for future PT scaffold research.<sup>22</sup> Various patterns of plasma treated PCL scaffolds produced by MEW have shown to be capable of sustaining a confluent layer of human umbilical cord vein derived smooth muscle cells.<sup>32</sup> These seeded cells showed a high cell viability and synthesis of collagen type I and III, and immunofluorescence imaging suggests the patterns in the PCL dictate cell alignment.<sup>32</sup> The ability of MEW produced PCL scaffolds to dictate cell alignment was also seen in endothelial cells.<sup>63</sup> In another study, MEW and SES were combined to create a bilayered tubular scaffold with an inner diameter of 3 mm, where the inner layer was produced by SES and seeded with endothelial colony forming cells and the outer layer was produced by MEW and seeded with MSCs. Since the bilayered design allowed the properties of the layers to be tailored to each cell type specifically, the outer layer contained circumferentially oriented fibers to dictate MSC orientation. In addition to the cell specific scaffold layers, the confluent cell layers allowed the use of cell specific medium on the inside and outside of the scaffold. The medium and fiber orientation used for the outer layer stimulated the differentiation of MSCs into elongated circumferentially oriented vSMC-like cells which coincided with a significant upregulation of calponin, (tropo)-elastin, and  $\alpha$ SMA.<sup>92</sup> As mentioned previously, the heating required for MES and MEW limits processing of natural polymers, leaving mostly synthetic polymers such as PCL<sup>32,63,93</sup> and polypropylene,<sup>94</sup> known for their relatively high hydrophobicity,<sup>31,58</sup> which may impact cell adhesion and solute transport. A recent study proposed (poly(hydroxymethylglycolide-*co*- $\epsilon$ -caprolactone) (pHMGCL) as a material option for MEW. pHMGCL is more hydrophilic than PCL and consequently more efficient in facilitating cell adhesion and dictating cell alignment of cardiac progenitor cells when compared to PCL.<sup>95</sup> All in all, MEW has a definite advantage when precise fiber deposition is desired.

**3.2. Near Field Electrospinning for Proximal Tubule Fabrication.** Another electrospinning technique with unique properties that could be valuable for PT scaffolds is near field electrospinning (NFES). It can use either molten or solution polymers, similar to MES and SES, respectively.<sup>57</sup> However, a lower voltage and collector distance is used in NFES, making it compatible with a wide variety of materials, which may even

contain living cells/bacteria that remain viable after deposition.<sup>57,96</sup> The relatively small distance between the spinneret and collector allows precise deposition of the polymer but also results in fibers that typically have a diameter in the micrometer range, although nanometer range has been reported.<sup>31,97,98</sup> One of the major limitations of NFES is the thickness of the scaffolds produced, which is typically in the range of 100  $\mu\text{m}$ –1 mm.<sup>31,96</sup> Although NFES has been used to demonstrate that human embryonic kidney cells are significantly impacted in their morphology by the alignment of deposited chitosan fibers,<sup>99</sup> to the best of our knowledge it has not yet been implemented in tubular scaffolds for *in vitro* nephron models.

Other fields have applied NFES to design constructs in which the technique is combined with 3D printing. For example, using small dispenser to collector distance and low voltage opens the possibility for electrospinning in near vicinity of live cells. Fattahi et al.<sup>91</sup> have created precisely programmed poly(methyl methacrylate) (PMMA) fiber patterns in a human mesenchymal stem cell (hMSC) loaded collagen hydrogel. The hMSCs in contact with a PMMA fiber would show an elongated morphology, which is different from the unidirectional spreading found in hMSCs that were not exposed to the fibers. For future research Fattahi et al. suggested adding an extruder to simultaneously deposit the collagen hydrogel and nanofibers, which could be used for highly customizable living bioscaffolds, such as blood vessels,<sup>91</sup> but potentially also renal grafts. In addition to the possibility of depositing fibers and bioink simultaneously, efforts have been made for direct electrospinning of fibers with live cells.<sup>36,57,96,100–102</sup> For this, certain parameters should be closely monitored in order to ensure that the intrafiber cells remain viable. Exposing cells to high voltages may disrupt their ion channels and gene expression or impact cell viability,<sup>36</sup> hence the voltage used for cell electrospinning is generally lower, which dictates the use of a lower dispenser to collector distance.<sup>36,57,100</sup> Compared to conventional SES configurations, which may alter the composition of their polymer solutions in order to manipulate fiber properties,<sup>35,83</sup> live cell solutions are rather limited in their configuration: First, the viscosity of the solution should be low to limit the shear stress imposed on cells during fiber formation and avoid damage. However, this is a fine line, since a certain minimal viscosity is required for the production of fibers. Shear stresses should also be considered when altering the dispenser flow rate.<sup>36</sup> Second, the solvents used in conventional SES are often cytotoxic, making them incompatible with living cell solutions. Although culture media can be used as solvent for electrospinning, this does limit the use of polymers to those that are water-soluble.<sup>100</sup> Finally, natural polymers are a logical choice from a cell viability perspective, but the resulting structures often have poor mechanical strength. The mechanical properties could be improved by incorporating a synthetic polymer, by, e.g., coaxial electrospinning, a layered design or a separate dispensing nozzle.<sup>36,58,100,101</sup>

Despite these limitations, electrospinning intrafiber live cells can successfully be achieved without reduction in cell viability. Nosoudi et al.<sup>100</sup> used a relatively low dispenser to collector distance and voltage for electrospinning a solution of gelatin/cells, gelatin/pullulan/cells, pullulan/cells, collagen/cells, and PEO/cells dissolved in culture media. The adipose tissue-derived stem cells (ASCs) electrospun with gelatin, pullulan, or both showed a cell viability not significantly different to that of

the control group, for which the same solutions were sprayed and cultured in a petri dish without voltage application. Furthermore, the electrospun cells did not show altered expression of SOX2 or OCT4 or increased cell death, indicating that the voltage exposure did not induce differentiation, loss of stemness, or reduced viability.<sup>100</sup> Townsend-Nicholson et al.<sup>101</sup> have shown that it is possible to employ coaxial electrospinning for encapsulation of live cells in media solution by an outer layer of PDMS. The EHDJ/1321N1 cells used in this study were incubated for 1 week postelectrospinning, after which they showed no significant difference compared to the control group in terms of cell viability, growth, and morphology.<sup>101</sup> In another study, ASCs electrospun with poly(vinyl alcohol) actually outperformed the sprayed control group after 28 days of incubation in proliferation and viability, while demonstrating the potential of live cell electrospinning.<sup>102</sup>

We have discussed the potential uses of MES/MEW and NFES as tools to fabricate a PT scaffold. Currently, research focusing on PT scaffolds has utilized solution electrospinning techniques only (Table 1). As outlined above, each system has its advantages and setbacks; however, taking a hybrid fabrication approach, drawing on the benefits of each system, will likely yield the greatest impact. An overview of the fabrication capabilities of each electrospinning system is provided in Table 3.

**Table 3. Overview of the Properties of Solution Electrospinning, Melt Electrospinning, Near-Field Electrospinning, Derived from the works of He et al.,<sup>57</sup> Kristen et al.,<sup>31</sup> and Ibrahim et al.<sup>58</sup>**

electrospinning type	tip-to-target distance (mm)	material form	fiber diameter ( $\mu\text{m}$ )	voltage (kV)
solution electrospinning	50–500	solution	0.01–5	10–30
melt electrospinning	50–500	melt	0.2–30	10–30
near-field electrospinning	0.5–5	solution/melt	0.05–60	0.05–12

## 4. CRITICAL ASPECTS TO CONSIDER WHEN DESIGNING A SYNTHETIC PROXIMAL TUBULE

**4.1. Fiber Diameter.** Based on the properties of the natural BM and the current knowledge of the performance of renal epithelial cells on electrospun scaffolds, there are some statements that can be made about the ideal scaffold properties of the inner layer. Although the luminal side of the scaffold supporting the epithelial cells should ideally resemble the natural BM, which mainly consists of 7 nm diameter natural fibers, epithelial cell viability was reportedly not significantly impacted by fiber diameter.<sup>77</sup> However, an increased fiber diameter gives rise to an increased pore size, which at some point reaches a critical tipping point where cells are unable to bridge the gaps and fail to form a confluent monolayer due to a lack of integrin-fiber contact and/or enforced maladapted cell morphology.<sup>22,75</sup> The fiber diameter at which this critical point is reached naturally depends on cell type and size and should be investigated further, although it is suggested that this critical point lies above 1  $\mu\text{m}$  for human renal epithelial cells.<sup>22,77</sup>

**4.2. Fiber Alignment.** The effect of fiber alignment on cell performance of PTECs is largely unknown and should be



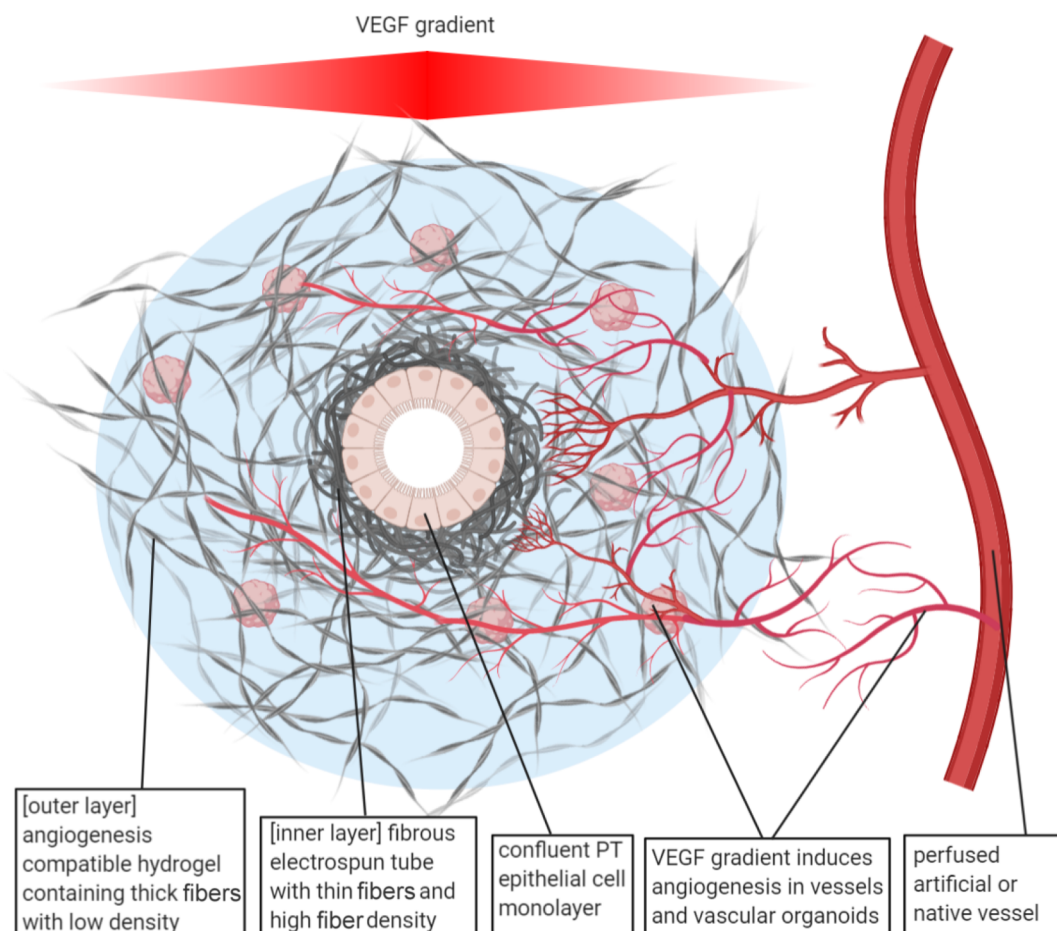


**Figure 3.** Schematic representation of the suggested PT tubule scaffold supporting ingrowth of capillaries. Scaffold layers, fibers, and cells are not to scale.

investigated. Human kidney epithelial cells seeded on randomly deposited PCL fibers with a diameter of roughly 1  $\mu\text{m}$  show a significantly higher gene expression of ANPEP, which is associated with PTECs because it regulates  $\text{Na}^+/\text{K}^+$ -ATPase expression,<sup>103</sup> when compared to controls made of TCPS. This difference was not significant between TCPS and PCL fibers with a similar diameter in an aligned formation.<sup>77</sup> This indicates that fiber orientation may have a larger impact on renal tubular cells fate than the material choice and therefore should be investigated further within a electrospinning strategy. The electrospinning methods most suitable for creating aligned fiber-based scaffolds are MEW and NFES, due to their high control of fiber deposition. However, these techniques generate relatively thick fibers (Table 3), which will make it difficult to replicate the 50 nm wave pattern seen in the natural BM.<sup>45</sup> While SES is less suitable for controlled deposition of fibers, it does require a relatively simple setup to create thin fibers and has acceptable material compatibility.

**4.3. Scaffold Material.** PCL is currently the most used material for developing electrospun artificial PTs (Table 1), and appears to perform well as long as the material's hydrophilicity is increased (e.g., by coating or plasma treatment) and the fiber diameter is sufficiently small.<sup>22,67,72,75,77</sup> An added benefit of using PCL is that the degradation mechanisms are well-described, including variants containing Upy or BU units, which allows for fine-tuning of degradation properties.<sup>60,67,68,81,86</sup> Considering the (well-known) properties of SES and PCL, it is no surprise these

are currently the most used in renal tubule modeling. We expect the SES-PCL scaffolds will remain a viable option for renal application, but considerable work is still required to identify the optimal fiber range, material stiffness, and degradation properties for this specific application. Meanwhile, new developments in other electrospinning techniques may open up the door to other materials that are more suitable for, e.g., MEW or NFES.

**4.4. Growth Factors.** Incorporating growth factors into the scaffold material could potentially enhance its performance. Vascular scaffolds have clearly demonstrated that incorporating growth factors for slow (*in situ*) release during the tissue expansion phase is effective,<sup>33,104,105</sup> and we believe these strategies should also be considered for renal scaffolds. Despite the fact that the mechanisms behind kidney regeneration are not yet fully understood, some growth factors, such as epidermal growth factor (EGF), VEGF, hepatocyte growth factor (HGF), and insulin-like growth factor 1 (IGF-1), have been identified as key components involved in kidney regeneration.<sup>106,107</sup> EGF supplementation to HK-2 cells *in vitro* resulted in increased VEGF secretion and subsequent cell proliferation,<sup>107</sup> making EGF a potentially interesting growth factor for addition to the scaffold material. VEGF has also been shown to stimulate proliferation and cell survival in immortalized rat PT cells.<sup>108</sup> Additionally VEGF plays an essential part in endothelial cell recruitment, stabilization, and proliferation<sup>109–111</sup> and could therefore be a valuable addition to promote and achieve vascularization of the PT scaffold. It

should be investigated if EGF could be used to create a sufficient VEGF gradient through secretion or if loading the scaffold with VEGF may be preferential. HGF influences ECM degradation by increasing expression of matrix metalloproteases that may impact the creation of a native BM by epithelial and vascular cells for replacement of the degradable scaffold. Moreover HGF is antiapoptotic and antifibrotic and contributes to stem cell recruitment *in vivo*.<sup>106</sup> Similarly, IGF-1 has also been shown to have antifibrotic and antiapoptotic effects.<sup>112,113</sup> Overall, the ability of (in)direct incorporation of VEGF or other growth factors to enhance PT scaffold performance should be studied.

**4.5. Vascularization of the PT.** The artificial PT scaffold should contain an outer layer designed for optimal vascular integration. The native nephron is surrounded by a peritubular vascular network that is crucial for the solute exchange with the bloodstream. It is therefore essential to not just optimize the inner lumen of the scaffold for a confluent layer of PT epithelial cells but also design an outer scaffold layer that supports and recruits capillary vessels in close proximity to the PT cells for optimal solute exchange. Recently, Wimmer et al.<sup>114</sup> developed a protocol to grow vascular organoids derived from (potentially autologous<sup>115</sup>) human iPSC. Organoids are multicellular structures cultured in 3D that have a microscale anatomy similar to its respective organ. These vascular organoids are capable of self-assembling into a stable and functional vascular network through multilineage differentiation.<sup>114</sup> Ideally, a combination of a VEGF gradient, vascular organoids, and perfused (artificial) vessels encased in a hydrogel environment generate a perfused capillary network that penetrates deep into the scaffold and exchanges solutes with the PT cells (Figure 3). This strategy requires a hybrid (electrospun scaffold/hydrogel) design in order to allow for remodeling of capillary structures in the hydrogel while also providing structural integrity provided by an electrospun frame. Electrospinning of hydrogel composites have successfully been used for creating vascularized constructs in other research areas.<sup>37,91,116,117</sup> Biocompatible hydrogels that have been used for capillary structure formation include collagen I, matrigel, and fibrin.<sup>118–120</sup> The electrospun structure in the layer should leave enough space for the hydrogel and organoids, while also containing fibers thick enough to supply the required structural support. Depending on the optimal fiber thickness, MEW could be a suitable method for electrospinning the outer layer due to its ability to precisely deposit microfibers. The vascular organoids to be embedded in this layer are not just capable of self-assembling into a vascular network but have previously been shown to be capable of developing connections with the (recipient's) native vessels.<sup>114</sup> This is critical because capillary connection with perfused (artificial) vessels is vital to ensure renal graft viability and function in both the bioreactor setup and *in vivo*. The use of vascular organoids or other microvascular fragments in the outer construct layer in combination with a VEGFA gradient is expected to be beneficial for multiple reasons. First, this strategy may realize a functional vascular network much faster than vascularization is purely reliant on angiogenesis via nearby already established perfused (macro)vessels. This is especially relevant *in vivo*, where the PT tubule construct requires swift vascularization to ensure connection to the recipient's vascular circulation and subsequent blood perfusion of the living tissue for survival. Second, seeded organoids could potentially be of autologous origin and therefore limit host versus donor

associated immune response complications.<sup>115,121</sup> Finally, for the development of a mature, stable microvessel with a confluent endothelial layer that is viable long-term, coculture with mural cells is also a requirement, which could be implemented by the use of organoids, which already contain microvascular structures composed of both ECs and mural cells, into the hydrogel.<sup>33,46,109,122</sup>

**4.6. Scaffold Performance.** Scaffold performance should be evaluated by monitoring cell viability, barrier function, transport function and scaffold degradation. Both the endothelium and epithelium should form a confluent monolayer with selective permeability. For the endothelial barrier function, tracer molecules of various sizes can be used to provide a benchmark,<sup>120</sup> while for PT cells the inulin permeability indicates whether or not a confluent epithelial layer is achieved.<sup>21,68</sup> Additionally, immunofluorescence should reveal the presence of cell junction markers VE-cadherin and ZO1 in ECs and PT cells, respectively.<sup>22,68,120</sup> The secretory function of PT cells can be evaluated by introducing fluorescent organic anions and cations to the basolateral side of the cells, with and without their respective transporter inhibitors.<sup>22</sup> A similar approach can be used to evaluate reabsorption of solutes, such as glucose.<sup>123</sup> Assessment of kidney function may require more complex bioreactor setups that are compatible with live imaging and uses separate flow systems for the endothelial and epithelial lumen.<sup>22,68,123</sup> Over time, the electrospun fibers are replaced by ECM as the scaffold degrades, and therefore, the polymer may have to contain Upy or BU units in order to match ECM secretion speed.<sup>60</sup> Supramolecular units such as PCL-Upy and PCL-BU can alter the PCL properties by speeding up degradation, inducing hydrogen bond stacking, and incorporating bioactive peptides.<sup>60,68,72,86</sup> Ideally, multiple scaffold materials, thicknesses, fiber densities, and fiber diameters are evaluated based on cell performance. While tuning scaffold properties, evaluation of performance should at least include measurements concerning confluency of the epithelial and endothelial monolayers under flow, uremic toxin secretion, and glucose reabsorption.

## 5. CONVERGING TECHNOLOGIES FOR NEXT GENERATION SYNTHETIC PROXIMAL TUBULE FABRICATION

Although this review focuses on the potential application of fiber-based technologies for the development of PT scaffolds, combining these manufacturing technologies with more cell-friendly fabrication methods, such as bioprinting, will likely yield more robust results with lasting applications in the clinic. The complexity and diversity of native tissue will eventually lead to the convergence of technologies in order to replicate this heterogeneity *in vitro*.<sup>124</sup> Using NFES with live cells does share some of the properties of electrospinning and bioprinting but at the cost of mechanical strength and product size limitations. However, recent developments in combining bioprinting and MEW for the fabrication of mechanically competent constructs that support cell growth and differentiation hold promise for applications in other fields.<sup>125</sup> Furthermore, the latest development in MEW nanoscale fibers in an automated and precise pattern allow the fabrication of biomimetic ECM structures to be constructed.<sup>88</sup> Convergence of such technologies will enable the construction of a whole tissue engineered functional kidney, with individual functional nephrons; supporting a plethora of cell and metabolic

functions. Overcoming the hurdles in integrating multiple fabrication technologies holds the key to multitechnology biofabrication.

## 6. CONCLUSION

The scarcity of donor kidneys and insufficient clearance of current dialysis techniques creates a need for cell loaded functional kidney scaffolds. We have given an overview of studies reporting on different electrospun scaffolds seeded with kidney epithelial cells. We also discussed how construct designs could be further improved by adopting other electrospinning methods and proposed a strategy for vascularization. Recent studies have shown the potential of electrospun scaffolds to support renal epithelial cells and their solute transport function, but have been limited to SES as a fabrication method. While SES has proven very effective for creating thin fibers, other methods such as MES, MEW, and NFES without solvents may also be considered as they offer higher spatial control during fiber deposition, or the possibility of intrafiber spinning of living cells. Inspired by the scaffold design strategies from the vascular field, we proposed a concept for an artificial PT tubule, consisting of a bilayered scaffold design containing growth factors. We argue that the inner layer should be thin and contain very fine fibers, to optimally support a confluent PTEC monolayer. The outer layer should contain a hydrogel that is structurally supported by a low fiber density network of thick fibers, which should be porous enough for capillary vessels to integrate into the scaffold and grow into close proximity of the PTECs. Considering the desired fiber structures, SES would be most fitting for the inner layer, whereas MES or MEW are most fitting for the outer layer. There are multiple growth factors that could be beneficial to the cellular development within the scaffold, of which VEGF appears to be the most promising. Further research is required in the field to study the feasibility and viability of these concepts and to fully integrate electrospinning technology into renal regenerative strategies. An intermediate step that produces a humanized *in vitro* testing platform for basic research and drug testing could be envisioned, before the desired functionality and complexity of the synthetic PTs is achieved for translation and implementation in clinical use. Thus, an electrospun synthetic PT would initially need to be designed with 3D *in vitro* testing in mind, i.e., for bioreactor applications, and would prove useful in, e.g., preclinical drug testing. In a potential second step, we envision future BAK devices to incorporate an electrospun synthetic PT to support epithelial cell function in order to address the current lack of reabsorptive and secretory functions in treatment options. Finally, to create a tissue engineered kidney, the proposed PT scaffold design could be scaled down to create functional nephron units enabling the addition of other renal cell types and structures. For this ultimate goal, we consider the *in vitro* bioreactor step to be critical for introducing convergence of the PT with the other sections of the functional nephron unit (e.g., the glomerulus) and for testing the boundaries concerning size reduction.

## AUTHOR INFORMATION

### Corresponding Author

**Caroline Cheng** – Department of Nephrology and Hypertension, University Medical Center Utrecht, 3508 GA Utrecht, The Netherlands; Experimental Cardiology, Department of Cardiology, Thorax Center, Erasmus

University Medical Center Rotterdam, 3015 GD Rotterdam, The Netherlands; Phone: +31 (0)-88-7557329; Email: K.L.Cheng-2@umcutrecht.nl; Fax: +31 (0)-88-7556283

### Authors

- Ijsbrand M. Vermue** – Department of Nephrology and Hypertension, University Medical Center Utrecht, 3508 GA Utrecht, The Netherlands
- Runa Begum** – Department of Nephrology and Hypertension, University Medical Center Utrecht, 3508 GA Utrecht, The Netherlands; [orcid.org/0000-0002-0466-8062](https://orcid.org/0000-0002-0466-8062)
- Miguel Castilho** – Department of Orthopaedics, University Medical Center Utrecht, 3508 GA Utrecht, The Netherlands; Regenerative Medicine Center Utrecht, 3508 GA Utrecht, The Netherlands; Department of Biomedical Engineering, Eindhoven University of Technology, 5612 AZ Eindhoven, The Netherlands; [orcid.org/0000-0002-4269-5889](https://orcid.org/0000-0002-4269-5889)
- Maarten B. Rookmaaker** – Department of Nephrology and Hypertension, University Medical Center Utrecht, 3508 GA Utrecht, The Netherlands
- Rosalinde Masereeuw** – Regenerative Medicine Center Utrecht, 3508 GA Utrecht, The Netherlands; Division of Pharmacology, Utrecht Institute for Pharmaceutical Sciences, Utrecht University, 3584 CS Utrecht, The Netherlands; [orcid.org/0000-0002-1560-1074](https://orcid.org/0000-0002-1560-1074)
- Carlijn V. C. Bouten** – Department of Biomedical Engineering and Institute for Complex Molecular Systems (ICMS), Eindhoven University of Technology, 5612 AZ Eindhoven, The Netherlands
- Marianne C. Verhaar** – Department of Nephrology and Hypertension, University Medical Center Utrecht, 3508 GA Utrecht, The Netherlands

Complete contact information is available at:  
<https://pubs.acs.org/10.1021/acsbomaterials.1c00408>

### Author Contributions

■ I.M.V. and R.B. have contributed equally to this work.

### Notes

The authors declare no competing financial interest.

### ACKNOWLEDGMENTS

This research was financially supported by the Gravitation Program “Materials Driven Regeneration”, funded by The Netherlands Organization for Scientific Research (024.003.013) and by the TKI-LSH funded project Biocompatible polymer scaffold design for the Renal reAbsorption unit (BIORAB). Figures were created with [BioRender.com](https://www.biorender.com).

### REFERENCES

- (1) Unglaub Silverthorn, D. *Human Physiology an Integrated Approach*, 6th ed.; Pearson, 2013.
- (2) Kramer, A.; Pippias, M.; Noordzij, M.; Stel, V. S.; Andrusev, A. M.; Aparicio-Madre, M. I.; Arribas Monzón, F. E.; Åsberg, A.; Barbullushi, M.; Beltrán, P.; Bonthuis, M.; Caskey, F. J.; Castro De La Nuez, P.; Cerneviskis, H.; De Meester, J.; Finne, P.; Golan, E.; Heaf, J. G.; Hemmeler, M. H.; Ioannou, K.; Kantaria, N.; Komissarov, K.; Korejwo, G.; Kramar, R.; Lassalle, M.; Lopot, F.; Macário, F.; Mackinnon, B.; Pálsson, R.; Pechter, Ú.; Piñera, V. C.; De Pablos, C. S.; Segarra-Medrano, A.; Seyahi, N.; Roblero, M. F. S.; Stojceva-Taneva, O.; Vazellov, E.; Winzeler, R.; Ziginiskiene, E.; Massy, Z.; Jager, K. J. The European Renal Association - European Dialysis and Transplant Association (ERA-EDTA) Registry Annual Report 2016: A Summary. *Clin. Kidney J.* **2019**, *12* (S), 702–720.



- (3) Salani, M.; Roy, S.; Fissell, W. H. Innovations in Wearable and Implantable Artificial Kidneys. *Am. J. Kidney Dis.* **2018**, *72* (5), 745–751.
- (4) Sirich, T. L.; Funk, B. A.; Plummer, N. S.; Hostetter, T. H.; Meyer, T. W. Prominent Accumulation in Hemodialysis Patients of Solutes Normally Cleared by Tubular Secretion. *J. Am. Soc. Nephrol.* **2014**, *25* (3), 615–622.
- (5) Lekawanvijit, S.; Kompa, A. R.; Krum, H. Protein-Bound Uremic Toxins: A Long Overlooked Culprit in Cardiorenal Syndrome. *Am. J. Physiol. - Ren. Physiol.* **2016**, *311* (1), F52–F62.
- (6) Masereeuw, R.; Mutsaers, H. A. M.; Toyohara, T.; Abe, T.; Jhawar, S.; Sweet, D. H.; Lowenstein, J. The Kidney and Uremic Toxin Removal: Glomerulus or Tubule? *Semin. Nephrol.* **2014**, *34* (2), 191–208.
- (7) Reiss, A. B.; Miyawaki, N.; Moon, J.; Kasselmann, L. J.; Voloshyna, L.; D'Avino, R.; De Leon, J. CKD, Arterial Calcification, Atherosclerosis and Bone Health: Inter-Relationships and Controversies. *Atherosclerosis* **2018**, *278* (November 2017), 49–59.
- (8) Sherman, R. A. Hyperphosphatemia in Dialysis Patients: Beyond Nonadherence to Diet and Binders. *Am. J. Kidney Dis.* **2016**, *67* (2), 182–186.
- (9) Atherton, J. G.; Hains, D. S.; Bissler, J.; Pendley, B. D.; Lindner, E. Generation, Clearance, Toxicity, and Monitoring Possibilities of Unaccounted Uremic Toxins for Improved Dialysis Prescriptions. *Am. J. Physiol. Renal Physiol.* **2018**, *315* (4), F890–F902.
- (10) Mair, R. D.; Sirich, T. L.; Meyer, T. W. Uremic Toxin Clearance and Cardiovascular Toxicities. *Toxins* **2018**, *10* (6), 226.
- (11) Wu, W.; Bush, K. T.; Nigam, S. K. Key Role for the Organic Anion Transporters, OAT1 and OAT3, in the in Vivo Handling of Uremic Toxins and Solutes. *Sci. Rep.* **2017**, *7* (1), 1–9.
- (12) Yamamoto, S. Molecular Mechanisms Underlying Uremic Toxin-Related Systemic Disorders in Chronic Kidney Disease: Focused on  $\beta$  2 -Microglobulin-Related Amyloidosis and Indoxyl Sulfate-Induced Atherosclerosis—Oshima Award Address 2016. *Clin. Exp. Nephrol.* **2019**, *23* (2), 151–157.
- (13) Locatelli, F.; La Milia, V.; Violo, L.; Del Vecchio, L.; Di Filippo, S. Optimizing Haemodialysate Composition. *Clin. Kidney J.* **2015**, *8* (5), 580–589.
- (14) Jansen, J.; Fedecostante, M.; Wilmer, M. J.; Peters, J. G.; Kreuser, U. M.; Van Den Broek, P. H.; Mensink, R. A.; Boltje, T. J.; Stamatalis, D.; Wetzels, J. F.; Van Den Heuvel, L. P.; Hoenderop, J. G.; Masereeuw, R. Bioengineered Kidney Tubules Efficiently Excrete Uremic Toxins. *Sci. Rep.* **2016**, *26715*.
- (15) Yousef Yengej, F. A.; Jansen, J.; Rookmaaker, M. B.; Verhaar, M. C.; Clevers, H. Kidney Organoids and Tubuloids. *Cells* **2020**, *9* (6), 1326.
- (16) van Gelder, M. K.; Mihaila, S. M.; Jansen, J.; Wester, M.; Verhaar, M. C.; Joles, J. A.; Stamatalis, D.; Masereeuw, R.; Gerritsen, K. G. F. From Portable Dialysis to a Bioengineered Kidney. *Expert Rev. Med. Devices* **2018**, *15* (5), 323–336.
- (17) Corridon, P. R.; Ko, I. K.; Yoo, J. J.; Atala, A. Bioartificial Kidneys. *Current Stem Cell Reports* **2017**, *3*, 68–76.
- (18) Ding, F.; Humes, H. D. The Bioartificial Kidney and Bioengineered Membranes in Acute Kidney Injury. *Nephron - Exp. Nephrol.* **2008**, *109* (4), e118.
- (19) Humes, H. D.; Weitzel, W. F.; Bartlett, R. H.; Swaniker, F. C.; Paganini, E. P.; Luderer, J. R.; Sobota, J. Initial Clinical Results of the Bioartificial Kidney Containing Human Cells in ICU Patients with Acute Renal Failure. *Kidney Int.* **2004**, *66* (4), 1578–1588.
- (20) Johnston, K. A.; Westover, A. J.; Rojas-Pena, A.; Buffington, D. A.; Pino, C. J.; Smith, P. L.; Humes, H. D. Development of a Wearable Bioartificial Kidney Using the Bioartificial Renal Epithelial Cell System (BRECS). *J. Tissue Eng. Regen. Med.* **2017**, *11* (11), 3048–3055.
- (21) Chevtchik, N. V.; Fedecostante, M.; Jansen, J.; Mihajlovic, M.; Wilmer, M.; Rützel, M.; Masereeuw, R.; Stamatalis, D. Upscaling of a Living Membrane for Bioartificial Kidney Device. *Eur. J. Pharmacol.* **2016**, *790*, 28–35.
- (22) Jansen, K.; Castilho, M.; Aarts, S.; Kaminski, M. M.; Lienkamp, S. S.; Pichler, R.; Malda, J.; Vermonden, T.; Jansen, J.; Masereeuw, R. Fabrication of Kidney Proximal Tubule Grafts Using Biofunctionalized Electrospun Polymer Scaffolds. *Macromol. Biosci.* **2019**, *19* (2), 1800412.
- (23) Gaal, R. C.; Fedecostante, M.; Fransen, P. P. K. H.; Masereeuw, R.; Dankers, P. Y.W. Renal Epithelial Monolayer Formation on Monomeric and Polymeric Catechol Functionalized Supramolecular Biomaterials. *Macromol. Biosci.* **2019**, *19* (2), 1800300.
- (24) Genderen, A. M.; Jansen, J.; Cheng, C.; Vermonden, T.; Masereeuw, R. Renal Tubular- and Vascular Basement Membranes and Their Mimicry in Engineering Vascularized Kidney Tubules. *Adv. Healthcare Mater.* **2018**, *7* (19), 1800529.
- (25) Schophuizen, C. M. S.; De Napoli, I. E.; Jansen, J.; Teixeira, S.; Wilmer, M. J.; Hoenderop, J. G. J.; Van Den Heuvel, L. P. W.; Masereeuw, R.; Stamatalis, D. Development of a Living Membrane Comprising a Functional Human Renal Proximal Tubule Cell Monolayer on Polyethersulfone Polymeric Membrane. *Acta Biomater.* **2015**, *14*, 22–32.
- (26) Hulshof, F.; Schophuizen, C.; Mihajlovic, M.; van Blitterswijk, C.; Masereeuw, R.; de Boer, J.; Stamatalis, D. New Insights into the Effects of Biomaterial Chemistry and Topography on the Morphology of Kidney Epithelial Cells. *J. Tissue Eng. Regen. Med.* **2018**, *12* (2), No. e817-e827.
- (27) Jansen, J.; De Napoli, I. E.; Fedecostante, M.; Schophuizen, C. M. S.; Chevtchik, N. V.; Wilmer, M. J.; Van Asbeck, A. H.; Croes, H. J.; Pertijs, J. C.; Wetzels, J. F. M.; Hilbrands, L. B.; Van Den Heuvel, L. P.; Hoenderop, J. G.; Stamatalis, D.; Masereeuw, R. Human Proximal Tubule Epithelial Cells Cultured on Hollow Fibers: Living Membranes That Actively Transport Organic Cations. *Sci. Rep.* **2015**, *5* (October), 1–12.
- (28) Katari, R.; Peloso, A.; Zambon, J. P.; Soker, S.; Stratta, R. J.; Atala, A.; Orlando, G. Renal Bioengineering with Scaffolds Generated from Human Kidneys. *Nephron - Exp. Nephrol.* **2014**, *126* (2), 119–124.
- (29) Orlando, G.; Farney, A. C.; Iskandar, S. S.; Mirmalek-Sani, S. H.; Sullivan, D. C.; Moran, E.; AbouShwareb, T.; Paolo, D. C.; Wood, K. J.; Stratta, R. J.; Atala, A.; Yoo, J. J.; Soker, S. Production and Implantation of Renal Extracellular Matrix Scaffolds from Porcine Kidneys as a Platform for Renal Bioengineering Investigations. *Ann. Surg.* **2012**, *256* (2), 363–370.
- (30) Nakayama, K. H.; Batchelder, C. A.; Lee, C. I.; Tarantal, A. F. Decellularized Rhesus Monkey Kidney as a Three-Dimensional Scaffold for Renal Tissue Engineering. *Tissue Eng., Part A* **2010**, *16* (7), 2207–2216.
- (31) Kristen, M.; Ainsworth, M. J.; Chirico, N.; van der Ven, C. F. T.; Doevendans, P. A.; Sluijter, J. P. G.; Malda, J.; van Mil, A.; Castilho, M. Fiber Scaffold Patterning for Mending Hearts: 3D Organization Bringing the Next Step. *Adv. Healthcare Mater.* **2020**, *9* (1), 1900775.
- (32) Saidu, N. T.; Wolf, F.; Bas, O.; Keijden, H.; Huttmacher, D. W.; Mela, P.; De-Juan-Pardo, E. M. Biologically Inspired Scaffolds for Heart Valve Tissue Engineering via Melt Electrowriting. *Small* **2019**, *15* (24), 1900873.
- (33) Han, F.; Jia, X.; Dai, D.; Yang, X.; Zhao, J.; Zhao, Y.; Fan, Y.; Yuan, X. Performance of a Multilayered Small-Diameter Vascular Scaffold Dual-Loaded with VEGF and PDGF. *Biomaterials* **2013**, *34* (30), 7302–7313.
- (34) Dos Santos, D. M.; Correa, D. S.; Medeiros, E. S.; Oliveira, J. E.; Mattoso, L. H. C. Advances in Functional Polymer Nanofibers: From Spinning Fabrication Techniques to Recent Biomedical Applications. *ACS Appl. Mater. Interfaces* **2020**, *12* (41), 45673–45701.
- (35) Ingavle, G. C.; Leach, J. K. Advancements in Electrospinning of Polymeric Nanofibrous Scaffolds for Tissue Engineering. *Tissue Eng., Part B* **2014**, *20* (4), 277–293.
- (36) Hong, J.; Yeo, M.; Yang, G. H.; Kim, G. Cell-Electrospinning and Its Application for Tissue Engineering. *Int. J. Mol. Sci.* **2019**, *20* (24), 6208.

- (37) Ekaputra, A. K.; Prestwich, G. D.; Cool, S. M.; Hutmacher, D. W. The Three-Dimensional Vascularization of Growth Factor-Releasing Hybrid Scaffold of Poly (E{open}-Caprolactone)/Collagen Fibers and Hyaluronic Acid Hydrogel. *Biomaterials* **2011**, *32* (32), 8108–8117.
- (38) Ziyadeh, F. N. Renal Tubular Basement Membrane and Collagen Type IV in Diabetes Mellitus. *Kidney Int.* **1993**, *43* (1), 114–120.
- (39) Halfter, W.; Oertle, P.; Monnier, C. A.; Camenzind, L.; Reyes-Lua, M.; Hu, H.; Candiello, J.; Labilloy, A.; Balasubramani, M.; Henrich, P. B.; Plodinec, M. New Concepts in Basement Membrane Biology. *FEBS J.* **2015**, *282* (23), 4466–4479.
- (40) Bhave, G.; Colon, S.; Ferrell, N. The Sulfilimine Cross-Link of Collagen IV Contributes to Kidney Tubular Basement Membrane Stiffness. *Am. J. Physiol. - Ren. Physiol.* **2017**, *313* (3), F596–F602.
- (41) Van Den Berg, F. Chapter 4.3-Extracellular Matrix. *Fascia: The Tensional Network of the Human Body*; Elsevier Ltd., 2012. DOI: 10.1016/B978-0-7020-3425-1.00058-1.
- (42) Yi, S.; Ding, F.; Gong, L.; Gu, X. Extracellular Matrix Scaffolds for Tissue Engineering and Regenerative Medicine. *Curr. Stem Cell Res. Ther.* **2017**, *12*, 233–246.
- (43) Maezawa, Y.; Cina, D.; Quaggin, S. *Seldin and Giebisch's The Kidney*; 1st ed.; Academic press, 2013; pp 721–755. DOI: 10.1016/C2009-0-62255-8.
- (44) Hohenester, E.; Yurchenco, P. D. Laminins in Basement Membrane Assembly. *Cell Adhesion & Migration* **2013**, *7*, 56–63.
- (45) Ogawa, S.; Ota, Z.; Shikata, K.; Hironaka, K.; Hayashi, Y.; Ota, K.; Kushiro, M.; Miyatake, N.; Kishimoto, N.; Makino, H. High-Resolution Ultrastructural Comparison of Renal Glomerular and Tubular Basement Membranes. *Am. J. Nephrol.* **1999**, *19* (6), 686–693.
- (46) Marchand, M.; Monnot, C.; Muller, L.; Germain, S. Extracellular Matrix Scaffolding in Angiogenesis and Capillary Homeostasis. *Semin. Cell Dev. Biol.* **2019**, *89* (August 2018), 147–156.
- (47) Miller, R. T. Mechanical Properties of Basement Membrane in Health and Disease. *Matrix Biol.* **2017**, *57–58*, 366–373.
- (48) Miner, J. H. Renal Basement Membrane Components. *Kidney Int.* **1999**, *56* (6), 2016–2024.
- (49) Chang, H. Y.; Kao, W. L.; You, Y. W.; Chu, Y. H.; Chu, K. J.; Chen, P. J.; Wu, C. Y.; Lee, Y. H.; Shyue, J. J. Effect of Surface Potential on Epithelial Cell Adhesion, Proliferation and Morphology. *Colloids Surf, B* **2016**, *141*, 179–186.
- (50) Brito, P. L.; Fioretto, P.; Drummond, K.; Kim, Y.; Steffes, M. W.; Basgen, J. M.; Sisson-Ross, S.; Mauer, M. Proximal Tubular Basement Membrane Width in Insulin-Dependent Diabetes Mellitus. *Kidney Int.* **1998**, *53* (3), 754–761.
- (51) Tyagi, I.; Agrawal, U.; Amitabh, V.; Jain, A.; Saxena, S. Thickness of Glomerular and Tubular Basement Membranes in Preclinical and Clinical Stages of Diabetic Nephropathy. *Indian J. Nephrol.* **2008**, *18* (2), 64–69.
- (52) Daniš, D.; Nyitrayová, O.; Slugeň, I.; Kováč, A.; Nyulassy, Š.; Orban, A. Tubular Basement Membrane Thickening in Diabetes Mellitus. *Int. Urol. Nephrol.* **1996**, *28* (4), 589–592.
- (53) Candiello, J.; Balasubramani, M.; Schreiber, E. M.; Cole, G. J.; Mayer, U.; Halfter, W.; Lin, H. Biomechanical Properties of Native Basement Membranes. *FEBS J.* **2007**, *274* (11), 2897–2908.
- (54) Chen, W. C.; Lin, H. H.; Tang, M. J. Regulation of Proximal Tubular Cell Differentiation and Proliferation in Primary Culture by Matrix Stiffness and ECM Components. *Am. J. Physiol. - Ren. Physiol.* **2014**, *307* (6), F695–F707.
- (55) Beamish, J. A.; Chen, E.; Putnam, A. J. Engineered Extracellular Matrices with Controlled Mechanics Modulate Renal Proximal Tubular Cell Epithelialization. *PLoS One* **2017**, *12* (7), e0181085.
- (56) Borza, C. M.; Chen, X.; Zent, R.; Pozzi, A. Cell Receptor-Basement Membrane Interactions in Health and Disease: A Kidney-Centric View. *Curr. Top. Membr.* **2015**, *76*, 231.
- (57) He, X. X.; Zheng, J.; Yu, G. F.; You, M. H.; Yu, M.; Ning, X.; Long, Y. Z. Near-Field Electrospinning: Progress and Applications. *J. Phys. Chem. C* **2017**, *121* (16), 8663–8678.
- (58) Ibrahim, Y. S.; Hussein, E. A.; Zagho, M. M.; Abdo, G. G.; Elzatahry, A. A. Melt Electrospinning Designs for Nanofiber Fabrication for Different Applications. *Int. J. Mol. Sci.* **2019**, *20* (10), 2455.
- (59) Wang, Z.; Mithieux, S. M.; Weiss, A. S. Fabrication Techniques for Vascular and Vascularized Tissue Engineering. *Adv. Healthcare Mater.* **2019**, *8* (19), 1900742.
- (60) van Haaften, E. E.; Duijvelshoff, R.; Ippel, B. D.; Söntjens, S. H. M.; van Houtem, M. H. C. J.; Janssen, H. M.; Smits, A. I. P. M.; Kurniawan, N. A.; Dankers, P. Y. W.; Bouten, C. V. C. The Degradation and Performance of Electrospun Supramolecular Vascular Scaffolds Examined upon in Vitro Enzymatic Exposure. *Acta Biomater.* **2019**, *92*, 48–59.
- (61) Şimşek, M.; Çapkin, M.; Karakeçili, A.; Günmünderelioğlu, M. Chitosan and Polycaprolactone Membranes Patterned via Electrospinning: Effect of Underlying Chemistry and Pattern Characteristics on Epithelial/Fibroblastic Cell Behavior. *J. Biomed. Mater. Res., Part A* **2012**, *100A* (12), 3332–3343.
- (62) Sobral, J. M.; Caridade, S. G.; Sousa, R. A.; Mano, J. F.; Reis, R. L. Three-Dimensional Plotted Scaffolds with Controlled Pore Size Gradients: Effect of Scaffold Geometry on Mechanical Performance and Cell Seeding Efficiency. *Acta Biomater.* **2011**, *7*, 1009–1018.
- (63) Bertlein, S.; Hikimoto, D.; Hochleitner, G.; Hümmer, J.; Jungst, T.; Matsusaki, M.; Akashi, M.; Groll, J. Development of Endothelial Cell Networks in 3D Tissues by Combination of Melt Electrospinning Writing with Cell-Accumulation Technology. *Small* **2018**, *14* (2), 1701521.
- (64) Pfeiffer, D.; Stefanitsch, C.; Wankhammer, K.; Müller, M.; Dreyer, L.; Krolitzki, B.; Zernetsch, H.; Glasmacher, B.; Lindner, C.; Lass, A.; Schwarz, M.; Muckenauer, W.; Lang, I. Endothelialization of Electrospun Polycaprolactone (PCL) Small Caliber Vascular Grafts Spun from Different Polymer Blends. *J. Biomed. Mater. Res., Part A* **2014**, *102* (12), 4500–4509.
- (65) Konopnicki, S.; Troulis, M. J. Mandibular Tissue Engineering: Past, Present, Future. *J. Oral Maxillofac. Surg.* **2015**, *73* (12), S136–S146.
- (66) Hohman, M. M.; Shin, M.; Rutledge, G.; Brenner, M. P. Electrospinning and Electrically Forced Jets. I. Stability Theory. *Phys. Fluids* **2001**, *13* (8), 2201–2220.
- (67) Chanda, A.; Adhikari, J.; Ghosh, A.; Chowdhury, S. R.; Thomas, S.; Datta, P.; Saha, P. Electrospun Chitosan/Polycaprolactone-Hyaluronic Acid Bilayered Scaffold for Potential Wound Healing Applications. *Int. J. Biol. Macromol.* **2018**, *116* (2017), 774–785.
- (68) Mollet, B. B.; Bogaerts, I. L. J.; van Almen, G. C.; Dankers, P. Y. W. A Bioartificial Environment for Kidney Epithelial Cells Based on a Supramolecular Polymer Basement Membrane Mimic and an Organotypical Culture System. *J. Tissue Eng. Regen. Med.* **2017**, *11* (6), 1820–1834.
- (69) Burton, T. P.; Callanan, A. A Non-Woven Path: Electrospun Poly(Lactic Acid) Scaffolds for Kidney Tissue Engineering. *Tissue Eng. Regen. Med.* **2018**, *15* (3), 301–310.
- (70) Schindler, M.; Ahmed, I.; Kamal, J.; Nur-E-Kamal, A.; Grafe, T. H.; Young Chung, H.; Meiners, S. A Synthetic Nanofibrillar Matrix Promotes in Vivo-like Organization and Morphogenesis for Cells in Culture. *Biomaterials* **2005**, *26* (28), 5624–5631.
- (71) Masaeli, E.; Morshed, M.; Rasekhan, P.; Karbasi, S.; Karbalaie, K.; Karamali, F.; Abedi, D.; Razavi, S.; Jafarian-Dehkordi, A.; Nasr-Esfahani, M. H.; Baharvand, H. Does the Tissue Engineering Architecture of Poly(3-Hydroxybutyrate) Scaffold Affects Cell-Material Interactions? *J. Biomed. Mater. Res., Part A* **2012**, *100* (7), 1907–1918.
- (72) Sobreiro-Almeida, R.; Fonseca, D. R.; Neves, N. M. Extracellular Matrix Electrospun Membranes for Mimicking Natural Renal Filtration Barriers. *Mater. Sci. Eng., C* **2019**, *103* (September 2018), 109866.



- (73) Duval, J.-L.; Dinis, T.; Vidal, G.; Vigneron, P.; Kaplan, D. L.; Egles, C. Organotypic Culture to Assess Cell Adhesion, Growth and Alignment of Different Organs on Silk Fibroin. *J. Tissue Eng. Regen. Med.* **2017**, *11* (2), 354–361.
- (74) Llorens, E.; Calderón, S.; Del Valle, L. J.; Puiggali, J. Polybiguanide (PHMB) Loaded in PLA Scaffolds Displaying High Hydrophobic, Biocompatibility and Antibacterial Properties. *Mater. Sci. Eng., C* **2015**, *50*, 74–84.
- (75) McHugh, K. J.; Tao, S. L.; Saint-Geniez, M. A Novel Porous Scaffold Fabrication Technique for Epithelial and Endothelial Tissue Engineering. *J. Mater. Sci.: Mater. Med.* **2013**, *24* (7), 1659–1670.
- (76) Ghasemi-Mobarakeh, L.; Morshed, M.; Karbalaie, K.; Fesharaki, M. A.; Nematollahi, M.; Nasr-Esfahani, M. H.; Baharvand, H. The Thickness of Electrospun Poly ( $\epsilon$ -Caprolactone Nanofibrous Scaffolds Influences Cell Proliferation. *Int. J. Artif. Organs* **2009**, *32* (3), 150–158.
- (77) Burton, T. P.; Corcoran, A.; Callanan, A. The Effect of Electrospun Polycaprolactone Scaffold Morphology on Human Kidney Epithelial Cells. *Biomed. Mater.* **2018**, *13* (1), 15006.
- (78) Romo-Urbe, A.; Meneses-Acosta, A.; Domínguez-Díaz, M. Viability of HEK 293 Cells on Poly- $\beta$ -Hydroxybutyrate (PHB) Biosynthesized from a Mutant *Azotobacter Vinelandii* Strain. Cast Film and Electrospun Scaffolds. *Mater. Sci. Eng., C* **2017**, *81*, 236–246.
- (79) Cameron, R. E.; Kamvari-Moghaddam, A. Synthetic Bioresorbable Polymers. *Durability and Reliability of Medical Polymers* **2012**, 96.
- (80) Woodruff, M. A.; Hutmacher, D. W. The Return of a Forgotten Polymer - Polycaprolactone in the 21st Century. *Prog. Polym. Sci.* **2010**, *35*, 1217.
- (81) Brugmans, M. C. P.; Söntjens, S. H. M.; Cox, M. A. J.; Nandakumar, A.; Bosman, A. W.; Mes, T.; Janssen, H. M.; Bouten, C. V. C.; Baaijens, F. P. T.; Driessen-Mol, A. Hydrolytic and Oxidative Degradation of Electrospun Supramolecular Biomaterials: In Vitro Degradation Pathways. *Acta Biomater.* **2015**, *27*, 21–31.
- (82) Kim, S.; Kim, G. H. Roles of Claudin-2, ZO-1 and Occludin in Leaky HK-2 Cells. *PLoS One* **2017**, *12* (12), e0189221.
- (83) Awad, N. K.; Niu, H.; Ali, U.; Morsi, Y. S.; Lin, T. Electrospun Fibrous Scaffolds for Small-Diameter Blood Vessels: A Review. *Membranes (Basel, Switz.)* **2018**, *8* (1), 15–26.
- (84) Radakovic, D.; Reboledo, J.; Helm, M.; Weigel, T.; Schürlein, S.; Kupczyk, E.; Leyh, R. G.; Walles, H.; Hansmann, J. A Multilayered Electrospun Graft as Vascular Access for Hemodialysis. *PLoS One* **2017**, *12* (10), e0185916.
- (85) Bonani, W.; Maniglio, D.; Motta, A.; Tan, W.; Migliaresi, C. Biohybrid Nanofiber Constructs with Anisotropic Biomechanical Properties. *J. Biomed. Mater. Res., Part B* **2011**, *96B* (2), 276–286.
- (86) Wang, X.; Shan, H.; Wang, J.; Hou, Y.; Ding, J.; Chen, Q.; Guan, J.; Wang, C.; Chen, X. Characterization of Nanostructured Ureteral Stent with Gradient Degradation in a Porcine Model. *Int. J. Nanomed.* **2015**, *10*, 3055–3064.
- (87) Yin, A.; Luo, R.; Li, J.; Mo, X.; Wang, Y.; Zhang, X. Coaxial Electrospinning Multicomponent Functional Controlled-Release Vascular Graft: Optimization of Graft Properties. *Colloids Surf., B* **2017**, *152*, 432–439.
- (88) Großhaus, C.; Bakirci, E.; Berthel, M.; Hrynevich, A.; Kade, J. C.; Hochleitner, G.; Groll, J.; Dalton, P. D. Melt Electrospinning of Nanofibers from Medical-Grade Poly( $\epsilon$ -Caprolactone) with a Modified Nozzle. *Small* **2020**, *16* (44), 2003471.
- (89) Deng, R.; Liu, Y.; Ding, Y.; Xie, P.; Luo, L.; Yang, W. Melt Electrospinning of Low-Density Polyethylene Having a Low-Melt Flow Index. *J. Appl. Polym. Sci.* **2009**, *114* (1), 166–175.
- (90) Dalton, P. D.; Klinkhammer, K.; Salber, J.; Klee, D.; Möller, M. Direct In Vitro Electrospinning with Polymer Melts. *Biomacromolecules* **2006**, *7* (3), 686–690.
- (91) Fattahi, P.; Dover, J. T.; Brown, J. L. 3D Near-Field Electrospinning of Biomaterial Microfibers with Potential for Blended Microfiber-Cell-Loaded Gel Composite Structures. *Adv. Healthcare Mater.* **2017**, *6* (19), 1700456.
- (92) Pennings, I.; van Haften, E. E.; Juengst, T.; Bultink, J. A.; Rosenberg, A. J. W. P.; Groll, J.; Bouten, C. V. C.; Kurniawan, N. A.; Smits, A. P. M.; Gawlitta, D. Layer-Specific Cell Differentiation in Bi-Layered Vascular Grafts under Flow Perfusion. *Biofabrication* **2020**, *12*, 015009.
- (93) Hochleitner, G.; Jünger, T.; Brown, T. D.; Hahn, K.; Moseke, C.; Jakob, F.; Dalton, P. D.; Groll, J. Additive Manufacturing of Scaffolds with Sub-Micron Filaments via Melt Electrospinning Writing. *Biofabrication* **2015**, *7* (3), 035002.
- (94) Mazalevska, O.; Struszczyk, M. H.; Krucinska, I. Design of Vascular Prostheses by Melt Electrospinning - Structural Characterizations. *J. Appl. Polym. Sci.* **2013**, *129* (2), 779–792.
- (95) Castilho, M.; Feyen, D.; Flandes-Iparraguirre, M.; Hochleitner, G.; Groll, J.; Doevendans, P. A. F.; Vermonden, T.; Ito, K.; Sluijter, J. P. G.; Malda, J. Melt Electrospinning Writing of Poly-Hydroxymethylglycolide-Co- $\epsilon$ -Caprolactone-Based Scaffolds for Cardiac Tissue Engineering. *Adv. Healthcare Mater.* **2017**, *6* (18), 1700311.
- (96) Li, X.; Li, Z.; Wang, L.; Ma, G.; Meng, F.; Pritchard, R. H.; Gill, E. L.; Liu, Y.; Huang, Y. Y. S. Low-Voltage Continuous Electrospinning Patterning. *ACS Appl. Mater. Interfaces* **2016**, *8* (47), 32120–32131.
- (97) Shin, D.; Kim, J.; Chang, J. Experimental Study on Jet Impact Speed in Near-Field Electrospinning for Precise Patterning of Nanofiber. *J. Manuf. Process.* **2018**, *36* (June), 231–237.
- (98) Chen, Q.; Mei, X.; Shen, Z.; Wu, D.; Zhao, Y.; Wang, L.; Chen, X.; He, G.; Yu, Z.; Fang, K.; Sun, D. Direct Write Micro/Nano Optical Fibers by near-Field Melt Electrospinning. *Opt. Lett.* **2017**, *42* (24), 5106–5109.
- (99) Fuh, Y.; Chen, S.; He, Z. Direct-Write, Highly Aligned Chitosan-Poly(Ethylene Oxide) Nanofiber Patterns for Cell Morphology and Spreading Control. *Nanoscale Res. Lett.* **2013**, *8* (1), 97.
- (100) Nosoudi, N.; Oommen, A. J.; Stultz, S.; Jordan, M.; Aldabel, S.; Hohne, C.; Mosser, J.; Archacki, B.; Turner, A.; Turner, P. Electrospinning Live Cells Using Gelatin and Pullulan. *Bioengineering* **2020**, *7* (1), 21.
- (101) Townsend-Nicholson, A.; Jayasinghe, S. N. Cell Electrospinning: A Unique Biotechnique for Encapsulating Living Organisms for Generating Active Biological Microthreads/Scaffolds. *Biomacromolecules* **2006**, *7* (12), 3364–3369.
- (102) Chen, H.; Liu, Y.; Hu, Q. A Novel Bioactive Membrane by Cell Electrospinning. *Exp. Cell Res.* **2015**, *338* (2), 261–266.
- (103) Kotlo, K.; Shukla, S.; Tawar, U.; Skidgel, R. A.; Danziger, R. S. Aminopeptidase N Reduces Basolateral Na<sup>+</sup>-K<sup>+</sup>-ATPase in Proximal Tubule Cells. *Am. J. Physiol. Renal Physiol.* **2007**, *293* (4), F1047–53.
- (104) Chiu, L. L. Y.; Radisic, M. Scaffolds with Covalently Immobilized VEGF and Angiopoietin-1 for Vascularization of Engineered Tissues. *Biomaterials* **2010**, *31* (2), 226–241.
- (105) Gao, C.; Harvey, E. J.; Chua, M.; Chen, B. P.; Jiang, F.; Liu, Y.; Li, A.; Wang, H.; Henderson, J. E. MSC-Seeded Dense Collagen Scaffolds with a Bolus Dose of VEGF Promote Healing of Large Bone Defects. *Eur. Cell. Mater.* **2013**, *26*, 195–207 discussion 207.
- (106) Flaquer, M.; Romagnani, P.; Cruzado, J. M. Factores de Crecimiento y Regeneración Renal. *Nefrología* **2010**, *30* (4), 385–393.
- (107) Zepeda-Orozco, D.; Wen, H. M.; Hamilton, B. A.; Raikwar, N. S.; Thomas, C. P. EGF Regulation of Proximal Tubule Cell Proliferation and VEGF-A Secretion. *Physiol. Rep.* **2017**, *5* (18), e13453.
- (108) Villegas, G.; Lange-Sperandio, B.; Tufro, A. Autocrine and Paracrine Functions of Vascular Endothelial Growth Factor (VEGF) in Renal Tubular Epithelial Cells. *Kidney Int.* **2005**, *67* (2), 449–457.
- (109) Reginato, S.; Gianni-Barrera, R.; Banfi, A. Taming of the Wild Vessel: Promoting Vessel Stabilization for Safe Therapeutic Angiogenesis. *Biochem. Soc. Trans.* **2011**, *39* (6), 1654–1658.
- (110) Rouwkema, J.; Khademhosseini, A. Vascularization and Angiogenesis in Tissue Engineering: Beyond Creating Static Networks. *Trends Biotechnol.* **2016**, *34* (9), 733–745.



(111) Udan, R. S.; Culver, J. C.; Dickinson, M. E. Understanding Vascular Development: WIRE Developmental Biology (2012). *Wiley Interdiscip. Rev. Dev. Biol.* **2013**, *2* (3), 327–346.

(112) Wu, Z.; Yu, Y.; Niu, L.; Fei, A.; Pan, S. IGF-1 Protects Tubular Epithelial Cells during Injury via Activation of ERK/MAPK Signaling Pathway. *Sci. Rep.* **2016**, *6*, 28066.

(113) Zhang, G.; Ichimura, T.; Maier, J. A.; Maciag, T.; Stevens, J. L. A Role for Fibroblast Growth Factor Type-1 in Nephrogenic Repair. Autocrine Expression in Rat Kidney Proximal Tubule Epithelial Cells in Vitro and in the Regenerating Epithelium Following Nephrotoxic Damage by S-(1,1,2,2-Tetrafluoroethyl)-L-Cysteine in V. *J. Biol. Chem.* **1993**, *268* (16), 11542–11547.

(114) Wimmer, R. A.; Leopoldi, A.; Aichinger, M.; Wick, N.; Hantusch, B.; Novatchkova, M.; Taubenschmid, J.; Hämmerle, M.; Esk, C.; Bagley, J. A.; Lindenhofer, D.; Chen, G.; Boehm, M.; Agu, C. A.; Yang, F.; Fu, B.; Zuber, J.; Knoblich, J. A.; Kerjaschki, D.; Penninger, J. M. Human Blood Vessel Organoids as a Model of Diabetic Vasculopathy. *Nature* **2019**, *565* (7740), 505–510.

(115) Song, B.; Cha, Y.; Ko, S.; Jeon, J.; Lee, N.; Seo, H.; Park, K.-J.; Lee, I.-H.; Lopes, C.; Feitosa, M.; Luna, M. J.; Jung, J. H.; Kim, J.; Hwang, D.; Cohen, B. M.; Teicher, M. H.; Leblanc, P.; Carter, B. S.; Kordower, J. H.; Bolshakov, V. Y.; Kong, S. W.; Schweitzer, J. S.; Kim, K.-S. Human Autologous iPSC - Derived Dopaminergic Progenitors Restore Motor Function in Parkinson's Disease Models Graphical Abstract Find the Latest Version: Human Autologous iPSC - Derived Dopaminergic Progenitors Restore Motor Function in Parkinson's d. *J. Clin. Invest.* **2019**, *130* (2), 904–920.

(116) Vedadghavami, A.; Minooei, F.; Mohammadi, M. H.; Khetani, S.; Rezaei Kolahchi, A.; Mashayekhan, S.; Sanati-Nezhad, A. Manufacturing of Hydrogel Biomaterials with Controlled Mechanical Properties for Tissue Engineering Applications. *Acta Biomater.* **2017**, *62*, 42–63.

(117) Li, X.; Cho, B.; Martin, R.; Seu, M.; Zhang, C.; Zhou, Z.; Choi, J. S.; Jiang, X.; Chen, L.; Walia, G.; Yan, J.; Callanan, M.; Liu, H.; Colbert, K.; Morrissette-McAlmon, J.; Grayson, W.; Reddy, S.; Sacks, J. M.; Mao, H.-Q. Nanofiber-Hydrogel Composite-Mediated Angiogenesis for Soft Tissue Reconstruction. *Sci. Transl. Med.* **2019**, *11* (490), eaau6210.

(118) Arnaoutova, I.; Kleinman, H. K. In Vitro Angiogenesis: Endothelial Cell Tube Formation on Gelled Basement Membrane Extract. *Nat. Protoc.* **2010**, *5* (4), 628–635.

(119) Chan, J. M.; Zervantonakis, I. K.; Rimchala, T.; Polacheck, W. J.; Whisler, J.; Kamm, R. D. Engineering of In Vitro 3D Capillary Beds by Self-Directed Angiogenic Sprouting. *PLoS One* **2012**, *7* (12), e50582.

(120) Bogorad, M. I.; DeStefano, J.; Wong, A. D.; Searson, P. C. Tissue-Engineered 3D Microvessel and Capillary Network Models for the Study of Vascular Phenomena. *Microcirculation* **2017**, e12360.

(121) Markou, M.; Kouroupis, D.; Badounas, F.; Katsouras, A.; Kyrkou, A.; Fotsis, T.; Murphy, C.; Bagli, E. Tissue Engineering Using Vascular Organoids From Human Pluripotent Stem Cell Derived Mural Cell Phenotypes. *Front. Bioeng. Biotechnol.* **2020**, *8* (April), 1–20.

(122) van Dijk, C. G. M.; Brandt, M. M.; Poullis, N.; Anten, J.; van der Moolen, M.; Kramer, L.; Homburg, E.; Louzao-Martinez, L.; Pei, J.; Krebber, M.; Van Balkom, B. W. M.; de Graaf, P.; Duncker, D. J.; Verhaar, M. C.; Luttgé, R.; Cheng, C. A New Microfluidic Model That Allows Monitoring of Complex Vascular Structures and Cell Interactions in a 3D Biological Matrix. *Lab Chip* **2020**, *20*, 1827.

(123) Lin, N. Y. C.; Homan, K. A.; Robinson, S. S.; Kolesky, D. B.; Duarte, N.; Moisan, A.; Lewis, J. A. Renal Reabsorption in 3D Vascularized Proximal Tubule Models. *Proc. Natl. Acad. Sci. U. S. A.* **2019**, *116* (12), 5399–5404.

(124) Castilho, M.; Ruijter, M.; De Beirne, S.; Villette, C. C.; Ito, K.; Wallace, G. G.; Malda, J. Multitechnology Biofabrication: A New Approach for the Manufacturing of Functional Tissue Structures? *Trends Biotechnol.* **2020**, *38*, 1316.

(125) de Ruijter, M.; Ribeiro, A.; Dokter, I.; Castilho, M.; Malda, J. Simultaneous Micropatterning of Fibrous Meshes and Bioinks for the

Fabrication of Living Tissue Constructs. *Adv. Healthcare Mater.* **2019**, *8*, 1800418.